

**ANALYSIS OF SPATIAL VARIABILITY OF  
ROCK-MASS QUALITY AND  
THERMAL-MECHANICAL EFFECTS IN GEOLOGIC  
DISPOSAL OF HIGH-LEVEL NUCLEAR WASTE**

*Prepared for*

**U.S. Nuclear Regulatory Commission  
Contract NRC-02-07-006**

*Prepared by*

**Goodluck Ofoegbu**

**Center for Nuclear Waste Regulatory Analyses  
San Antonio, Texas**

**September 2011**

## ABSTRACT

This report describes analyses performed from March 1998 through April 1999 to examine the effects of spatial variability of rock-mass quality on thermal-mechanical effects in geologic disposal of high-level nuclear waste. Spatial variability of rock-mass quality based on mapped fracture data is represented in complementary site- and drift-scale numerical finite element models of a conceptual waste disposal design. Analyses performed using the models indicate that a vertical temperature gradient centered at the disposal horizon combines with weaker lateral temperature gradients to create stress conditions that could favor rock damage close to disposal openings and in intervening pillars. Rock damage in the roof and floor of the openings could be reduced using appropriate ground support and is likely to occur more in rock of lower mechanical quality. However, ground support would not affect potential rock damage in the pillar, because such damage is driven by stress conditions outside the influence zone of typical ground support. Because of the stress control, rock damage in the pillar could occur more in rock of higher mechanical quality. The results show that ground support could be effective in stabilizing an underground opening used for disposal of high-level nuclear waste, if the ground support system is designed to withstand loading due to suppressed inelastic deformation and thermal expansion of the support elements and supported rock.

# CONTENTS

Section	Page
ABSTRACT .....	ii
FIGURES .....	iv
TABLE .....	vi
ACKNOWLEDGMENTS .....	vii
1 INTRODUCTION.....	1-1
2 ROCK-MASS QUALITY DATA .....	2-1
3 MODEL DESCRIPTION .....	3-1
3.1 Model Geometry and Finite Element Discretization .....	3-1
3.2 Material Models and Properties.....	3-1
3.3 Initial and Boundary Conditions and Heat Source.....	3-4
3.4 Analysis Procedure .....	3-4
4 CALCULATED THERMAL-MECHANICAL RESPONSE.....	4-1
4.1 Host Rock Temperature .....	4-1
4.2 Rock Damage Based on Inelastic Strain .....	4-1
4.3 Modeling with Single-Valued Rock-Mass Quality Index .....	4-10
4.4 Effects of Ground Support on Rock Damage .....	4-11
4.5 Potential Loading of a Concrete Liner Ground Support.....	4-14
5 SUMMARY OF INSIGHTS .....	5-1
6 REFERENCES.....	6-1

## FIGURES

Figures	Page
1-1	Layout of the Conceptual Disposal Design (From DOE Figure 4-22, 1998) ..... 1-3
2-1	Distribution of Rock-Mass Quality Q Along the Eastern Boundary of the Conceptual Disposal Drift Array of DOE Figure 4-22 (1988) Based on the “Full-Peripheral Data” Described in a DOE Contractor Report CRWMS M&O Figure 40, 1997a)..... 2-2
3-1	Schematic Illustration of the Site-Scale Model Showing a 2,800-m Wide Disposal Drift Array at a Depth of 300 m Below the Ground Surface ..... 3-2
3-2	Geometry and Finite Element Discretization of the Drift-Scale Model ..... 3-3
3-3	History of Total Heat Source $S_n$ Used To Represent the Thermal Load of Disposed Nuclear Waste Based on CRWMS M&O Table V-1 (1997b) ..... 3-5
4-1	Temperature Distributions Over the Conceptual Disposal Array at 25, 50, 100, and 150 Years After Instantaneous Waste Loading of All Disposal Drifts..... 4-2
4-2	Temperature Distributions Within Approximately 100 m Above and Below the First 10 Disposal Drifts at the South End of the Site-Scale Model (Drifts #91–100) at 50 and 150 Years After Instantaneous Waste Loading of All Disposal Drifts..... 4-3
4-3	Temperature Distributions Within 25 m Above and Below a Drift Based on the Drift-Scale Model at 150 Years After Instantaneous Waste Loading of All Disposal Drifts ..... 4-4
4-4	Inelastic Strain Distribution at 150 Years for the Case of Drift Openings With Stiff Ground Support. The Plot Arrangement is the Same as Described in Figure 2-1 ..... 4-5
4-5	Inelastic Strain Distribution at 150 Years for the Case of Drift Openings With Degraded Ground Support. The Plot Arrangement is the Same as Described in Figure 2-1 ..... 4-6
4-6	Inelastic Strain Distribution at 150 Years Based on the Drift-Scale Model for Areas of High Rock-Mass Quality..... 4-7
4-7	Inelastic Strain Distribution at 150 Years Based on the Drift-Scale Model for Areas of Low Rock-Mass Quality ..... 4-8
4-8	Schematic Illustration of Rock Deformation Mechanisms Due to Heat From a Horizontal Array of Fully Loaded Waste Disposal Drifts ..... 4-9
4-9	Inelastic Strain Distributions Between Drift Numbers 91–100 (at the South End of the Disposal Array) Calculated Using Three Model Cases ..... 4-11
4-10	Inelastic Strain Distributions Between Drift Numbers 41–50 (in the Middle of the Disposal Array) Calculated Using Three Model Cases..... 4-12
4-11	Displacement History at the Roof, Floor, and North and South Sidewalls of a Disposal Drift Without Ground Support Based on a Drift-Scale Model Analysis for High-Q Areas ..... 4-13
4-12	Inelastic Strain Distributions at 150 Years Based on Drift-Scale Modeling for High-Q Areas, Showing the Effects of Ground Support on Thermally Induced Rock Damage ..... 4-15
4-13	Distribution of Liner Pressure Around a Drift Circumference at 150 Years After Instantaneous Waste Loading, Based on Highest-Q and Lowest-Q Drift-Scale Models With Liner Fully Bonded to Rock ..... 4-16
4-14	Variation of Liner Pressure With Angular Distance Around a Drift Circumference at 150 Years After Instantaneous Waste Loading, Based on Highest-Q and Lowest-Q Drift-Scale Models With Liner Fully Bonded to Rock ..... 4-17

## FIGURES (continued)

Figures	Page
4-15 Effects of the Liner-Rock Interface Model on the Calculated Liner Pressure Showing Results for a Fully-Bonded Interface Model and a Frictional-Interface Model With a Friction Coefficient of 0.6 .....	4-18

## TABLES

Tables		Page
3-1	Relationship Between Thermal Expansivity and Temperature.....	3-3
3-2	Sequence of Thermal and Mechanical Analyses .....	3-5
4-1	Vertical Thickness of Rock Subjected to Given Temperature Ranges at 150 Years Based on the Site-Scale (Figure 4-2, lower plot) and Drift-Scale [Figure 4-3(a)] Models .....	4-4

## ACKNOWLEDGMENTS

This report describes work performed by the Center for Nuclear Waste Regulatory Analyses (CNWRA<sup>®</sup>) and its contractors for the U.S. Nuclear Regulatory Commission (USNRC) under Contract No. NRC-02-07-006. The activities reported here were performed on behalf of the USNRC Office of Nuclear Material Safety and Safeguards, Division of High-Level Waste Repository Safety. This report is an independent product of CNWRA and does not necessarily reflect the view or regulatory position of USNRC.

The author gratefully acknowledges B. Dasgupta for his technical review, E. Pearcy for his programmatic review and editorial review, and A. Ramos for her administrative support. Furthermore, the author gratefully acknowledges E. Pearcy and J. McMurry for encouraging him to search previous scientific notebooks for unpublished work.

## QUALITY OF DATA, ANALYSES, AND CODE DEVELOPMENT

**DATA:** All CNWRA-generated original data contained in this report meet the quality assurance requirements described in the Geosciences and Engineering Division Quality Assurance Manual. Sources for other data should be consulted for determining the level of quality for those data. Computational calculations described in this report have been recorded in CNWRA Scientific Notebook Nos. 263 (Ofoegbu, 2008a) and 321 (Ofoegbu, 2000) and have been described in previous CNWRA publications (Ofoegbu, 1998b, 1999).

### References

Ofoegbu, G.I. "Repository Scale Thermal-Merchanical 2-D Model." Scientific Notebook No. 321. San Antonio, Texas: Center for Nuclear Waste Regulatory Analyses. 2000.

Ofoegbu, G.I. "Variations of Drift Stability at the Proposed Yucca Mountain Repository." Proceedings of the 37<sup>th</sup> U.S. Rock Mechanics Symposium, June 6-9, 1999. Vail, Colorado: Rock Mechanics for Industry. 1999.

Ofoegbu, G.I. "Repository Scale Thermal-Merchanical Model." Scientific Notebook No. 263. San Antonio, Texas: Center for Nuclear Waste Regulatory Analyses. 2008a.

Ofoegbu, G.I. "Effects of Spatial and Temporal Variations of Rock-Mass Quality and Integrity of Support on Distributions of Potential Instability at the Proposed Yucca Mountain Repository for High-Level Nuclear Waste." San Antonio, Texas: CNWRA. 1998b.

# 1 INTRODUCTION

The potential for occurrence of a zone of damaged rock around underground openings used for geologic disposal of high-level radioactive waste is a key consideration for the disposal system design. Rock within the zone is referred to as damaged in the sense that the capability of the rock to contribute to waste isolation may have degraded somewhat by the formation of a fracture or crack population that did not exist prior to the excavation, waste emplacement, or other activities related to the repository development. The rock is considered damaged relative to the initial state because of the effects of the fractures or cracks on mechanical load-bearing capacity or on water flow. For example, Tsang, et al. (2005) defined the damaged zone as a zone in which the flow and transport properties of the rock have changed significantly relative to the initial rock-mass condition. However, defining rock damage with respect to the hydrological or mechanical effect could complicate damage characterization because a damage intensity great enough to cause a hydrological effect may be insignificant to mechanical stability. Therefore, in this work damage intensity is described in terms of the magnitude of inelastic strain, which could be used to derive indices for characterizing the hydrological or mechanical effects.

Damage due to cracks or fractures is a characteristic of brittle rocks that have low matrix porosity or permeability but may support fluid flow through a network of cracks or fractures. As Tsang, et al. (2005) described, other forms of damage, such as pore dilation, may occur in other rock types. In brittle rocks, damage is triggered by stress changes large enough to overcome the rock strength. Such a stress change may result from excavation, thermal loading, or water pressure change. However, discussion and evaluations of rock damage around excavations typically have been dominated by consideration of damage due to excavation. There have been numerous references to the excavation damaged zone (EDZ) and several international meetings and activities aimed at understanding the characteristics of the EDZ, such as those Tsang, et al. (2005) described. In contrast, rock damage due to thermal load has not received much attention, though the extent and duration of significant temperature change due to disposed radioactive waste suggest that thermally induced damage could be significant. For example, Andersson (2007) described *in-situ* heater test results that show rock spalling due to a simulated thermal load in a shaft in granitic rock was approximately three times the spalling caused by excavation of the shaft.

Rock deformation due to thermal load could consist of free thermal expansion or a response to the stress change due to suppressed thermal expansion. The latter occurs if the rock is heated nonuniformly and, consequently, tries to expand by different amounts at neighboring points. Nonuniform heating of the host rock of a geologic repository is inevitable because nuclear waste containers with varying heat output capacities are placed at discrete locations in the rock at discrete times, and heat produced by each container flows into the rock at a finite rate controlled by the host rock thermal conductivity. Consequently, the host rock is heated by an amount that varies spatially and temporally. Therefore, potential expansion of the rock is partially suppressed by different amounts in different directions due to neighborhood resistance, resulting in nonuniform increase in rock stress. The rock deforms as a result of adjusting to a new equilibrium state. Additionally, the thermal load causes pore fluids to try to expand by different amounts at neighboring points because of spatially varying temperature, which results in fluid pressure increase if the fluids cannot flow freely. The excess fluid pressure causes a change in the rock stress and loading conditions, and the rock deforms to adjust to a new equilibrium state. The excess pore pressure dissipates with time at a rate that depends on the fluid conductivities, compressibility of the solids skeleton, and distance to drainage boundaries.

Rock deformations can be elastic and therefore fully reversible, or they can be inelastic. Inelastic deformations may manifest through formation of new cracks, slip or opening or closing of existing cracks, or particle morphology changes not associated with cracking. In brittle rocks, such as various types of igneous, metamorphic, and indurated sedimentary rocks, inelastic deformation is dominated by cracking and is associated with damage because of the effect on mechanical strength and stiffness and on rock characteristics important to waste isolation, such as hydrologic and transport properties.

The intensity and extent of thermally induced damage depend on the thermal load and rock-mass thermal and mechanical properties. The thermal load and rock-mass thermal properties determine the magnitude and gradients of temperature, which combine with the rock-mass stiffness to determine the thermal stress, as Timoshenko and Goodier (1970, Chapter 13, Article 153) explained. The rock-mass strength determines damage occurrence for a given stress state.

The work described in this report was performed from March 1998 through April 1999 to examine how the effects of spatial variability of rock-mass mechanical properties may affect thermally induced damage. The analyses were based on a conceptual design by the U.S. Department of Energy (DOE) for geologic disposal of radioactive waste at Yucca Mountain, Nevada (DOE, 1998, Figure 4-22). The conceptual design considered a horizontal array of waste disposal drifts approximately normal to an access main tunnel (Figure 1-1). The access tunnel in the conceptual design coincided with an existing tunnel that DOE had excavated to provide access for exploration of the rock-mass being considered as host rock of the disposal openings. Fracture data from the walls of the exploratory tunnel were used to estimate values of the rock-mass quality,  $Q$ , index as described in Civilian Radioactive Waste Management System Management and Operating Contractor (CRWMS M&O) (1997a, Figure 40). For the work described in this report, the  $Q$  data were used to define a potential variation of the rock-mass strength and stiffness in the north-south direction along the access tunnel based on a procedure Hoek and Brown (1997) described. The resulting mechanical property variation was projected uniformly in the east-west direction along the disposal drifts and, therefore, was assumed to apply to the entire host rock-mass of the conceptual design. The mechanical property variation was used to calculate variations of thermally induced rock damage in the north-south direction among the disposal drifts. The evaluation of rock damage focused on the mechanical effects of thermal expansion of solids but did not include any effects due to thermal expansion of water or air.

Spatial relationships among the  $Q$  data, exploratory tunnel, and conceptual disposal drift array are described in Chapter 2 of this report. Chapter 3 describes the finite element models used for the analyses, and Chapter 4 describes the calculated results. Insights based on the analyses are summarized in Chapter 5.

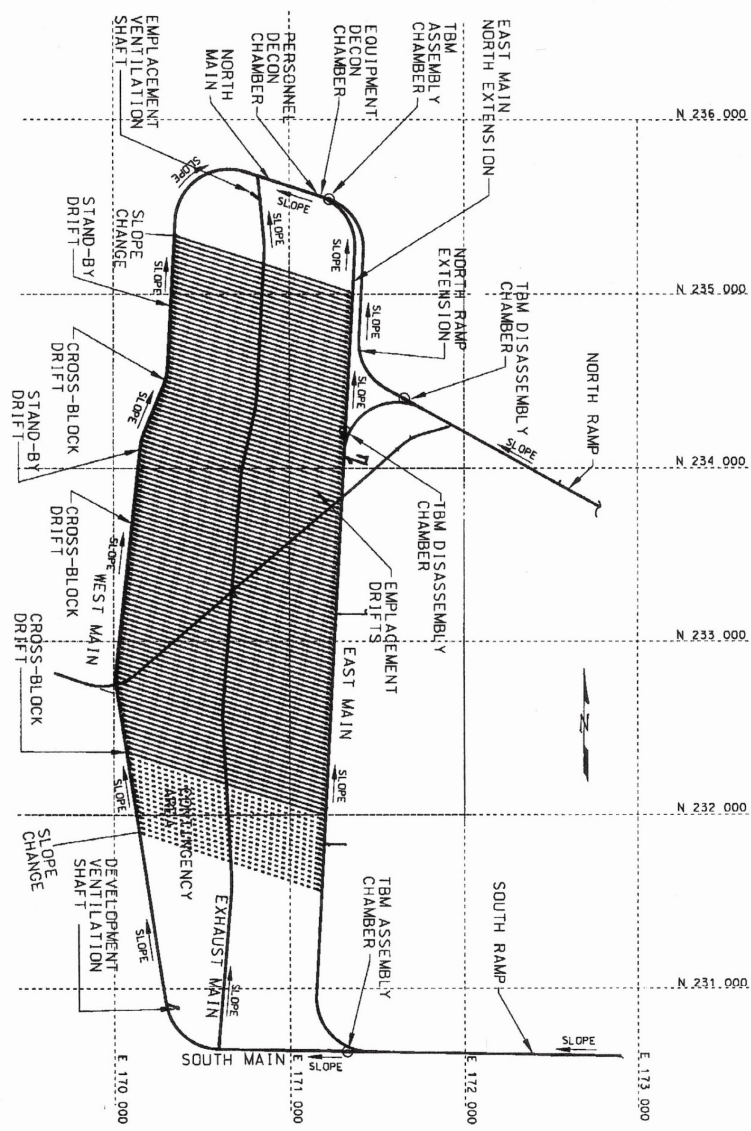


Figure 1-1. Layout of the Conceptual Disposal Design (From DOE, 1998, Figure 4-22)

## 2 ROCK-MASS QUALITY Q DATA

The exploratory tunnel, as described in DOE (1998, Figure 4-22), consists of a gently sloping north-south tunnel segment (east main) connected to the ground surface through the “north ramp” at the north and “south ramp” at the south. In the conceptual design (Figure 1-1), the east main connects to the eastern end of a series of disposal drifts oriented approximately east-west. The disposal drifts form a horizontal array. The eastern boundary of the array coincides with the east main but extends approximately 1 km [0.62 mi] to the north beyond the east main. The exploratory tunnel (east main and north and south ramps) covers a total distance of approximately 8 km [5 mi]. In the conceptual design, the disposal array consists of 105 drifts spaced at 28 m [91.9 ft] center to center. The drift array occupies a distance of approximately 2 km [1.24 mi] along the east main and approximately 1 km [0.62 mi] beyond the north end of the tunnel (Figure 1-1). The Q data cover the entire exploratory tunnel as shown in CRWMS M&O (1997a, Figure 40). Therefore, because of the geometrical relationship between the exploratory tunnel and the conceptual disposal array, the Q data cover the east boundary of approximately the southern two-thirds of the disposal array.

For modeling described in this report, the Q data were projected uniformly westward to the western end of the disposal array, the value at the north end of the east main (Figure 1-1) was projected uniformly northward to the end of the array, and all Q values were projected uniformly in the vertical direction. The implications of the spatial projections of the Q data will be discussed subsequently under “Model Description.” The resulting north-south (i.e., normal to the disposal drift array) variation of Q values is described in Figure 2-1. The model domain is a vertical north-south rectangle normal to the disposal drifts. Figure 2-1 illustrates the variation of Q values within a 35-m [115-ft]-high strip normal to the drifts and centered on the drift axis, each drift represented by a 5-m [16.4-ft]-high opening (white squares in Figure 2-1). To facilitate presentation, the strip is divided into 10 segments, each representing 10 drifts according to the numbers shown at the beginning and end of each segment in Figure 2-1. Drift number 100 is at the south end of the modeled array, and drift number 1 is at the north end. As described earlier, the Q value for drift number 32 (corresponding to the north end of the east main) was projected uniformly northward to obtain Q values for drift numbers 1–31 because of the lack of Q data for the northern one-third of the conceptual disposal array. The Q values in Figure 2-1 were based on the “full-peripheral data” of CRWMS M&O (1997a, Figure 40).

As Figure 2-1 shows, the rock-mass quality index attains maximum values in the middle of the array between drift numbers 31–70. The value of Q attains a maximum of approximately 13.6 between drift numbers 47 and 48 and a minimum of approximately 0.73 between drift numbers 98 and 99. The spatial variation of Q values depicted in Figure 2-1 was incorporated explicitly into a numerical finite element model as described in Chapter 3.

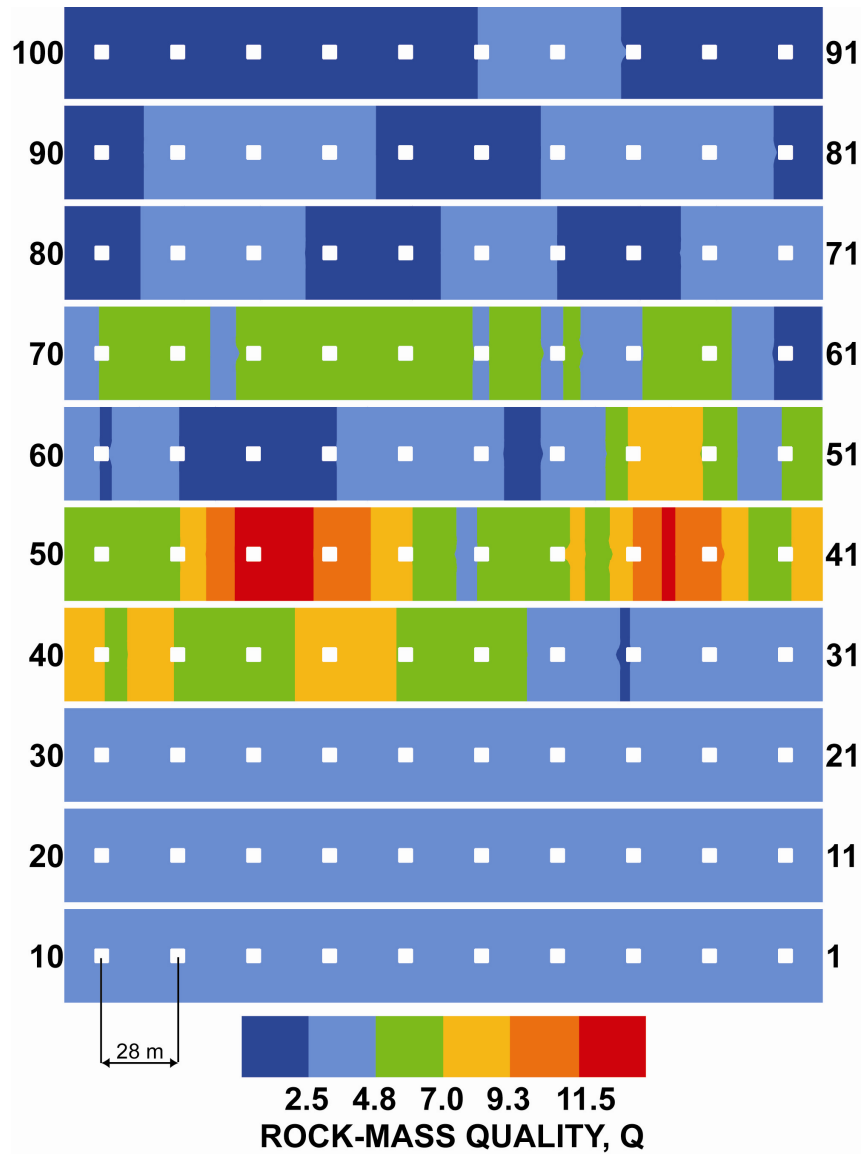


**Figure 2-1. Distribution of Rock-Mass Quality Q Along the Eastern Boundary of the Conceptual Disposal Drift Array of DOE (1988, Figure 4-22) Based on the “Full-Peripheral Data” Described in CRWMS M&O (1997a, Figure 40). The Figure Shows a 35-m [114.8-ft]-High Strip Centered on the Drift Axis. The Strip is Divided Into 10 Segments, Each Representing 10 Drifts (White Squares) According to the Numbers Shown at the Beginning and End of Each Segment. Drift Number 100 Is at the South End of the Array, and Number 1 Is at the North End.**

## 3 MODEL DESCRIPTION

### 3.1 Model Geometry and Finite Element Discretization

Analyses were performed at two spatial scales. A site-scale model that includes the entire disposal drift array was used to study potential variations of thermal-mechanical response within the array, and a drift-scale model was used to study the response at the spatial scale of an individual drift. The site-scale model (Figure 3-1) consists of a vertical north-south rectangle normal to the drift axis of the conceptual disposal array. The rectangle is 3,200 m [10,499 ft] wide in the north-south direction {i.e., 2,800 m [9,186 ft]} representing 100 drifts, plus a 200-m [656-ft] extension at the north and south ends, and is 1,000 m [3,281 ft] high. Each drift was represented in the site-scale model as a 5-m [16.4-ft] square opening with center (i.e., intersection with drift axis) at a depth of 302.5 m [992.4 ft] below the ground surface.

The drift-scale model (Figure 3-2) consists of a 28-m [92-ft]-wide by 195-m [640-ft]-high rectangle with spatial coordinates consistent with the site-scale model, as described in Figure 3-2(a). The model extends 95 m [312 ft] vertically above the roof and below the floor of a 5-m [16.4-ft]-diameter circular opening that represents the drift. The site-scale model was used to calculate temperature and displacement histories at the top, base, and left and right sides of the drift-scale model. Subsequently, the calculated histories from the site-scale model were used to define boundary conditions for the drift-scale model.

The site-scale and drift-scale models were based on plane strain idealization, which assumes that mechanical properties do not vary in the drift direction and *in-situ* stress components are normal and parallel to the drift axes. These assumptions permit modeling to examine the effects of mechanical property variability (using the modeled north-south variation) on damage intensity and extent. The modeling is expected to lead to insights regarding how thermally induced rock damage may vary among relatively high and low quality areas within a rock-mass, even if the results do not directly quantify the damage intensity and extent for any individual site.

The finite element models are based on eight-node quadrilateral elements with reduced integration and occasional six-node triangles for mesh refinement (e.g., Figure 3-2). For the site-scale model, beam elements with high stiffness were placed at the edges of the drift openings to represent a concrete liner ground support. In the drift-scale models, a 20-cm [7.9-in]-thick ring of material around the 5-m [16.4-ft]-diameter circle [shown in Figure 3-2(c) as two rings of solid elements] was assigned properties of concrete to represent a concrete liner ground support. The interface between the concrete liner elements and surrounding rock was modeled as fully bonded, except for the model variation described in Section 4.5 where the interface was modeled as frictional. In another variation of the drift-scale model described in Section 4.4, the 20-cm [7.9-in]-thick ring was fully bonded to and assigned the same properties as the surrounding rock to simulate a 5-m [16.4-ft]-diameter circular opening without ground support.

### 3.2 Material Models and Properties

Heat flow was simulated based on thermal conduction and using material properties from CRWMS M&O (1997b). The report gave a rock density of 2,274 kg/m<sup>3</sup> [142 lb/ft<sup>3</sup>]; thermal conductivity of 2.1 J/s.m.K; and a specific heat capacity of approximately 2.14, 10.5, or 2.18 MJ/m<sup>3</sup>.K at a temperature of 25–94, 94–114, or greater than 114 °C [77–201, 201–237, or greater than 237 °F], respectively. The increased specific heat value in the temperature range

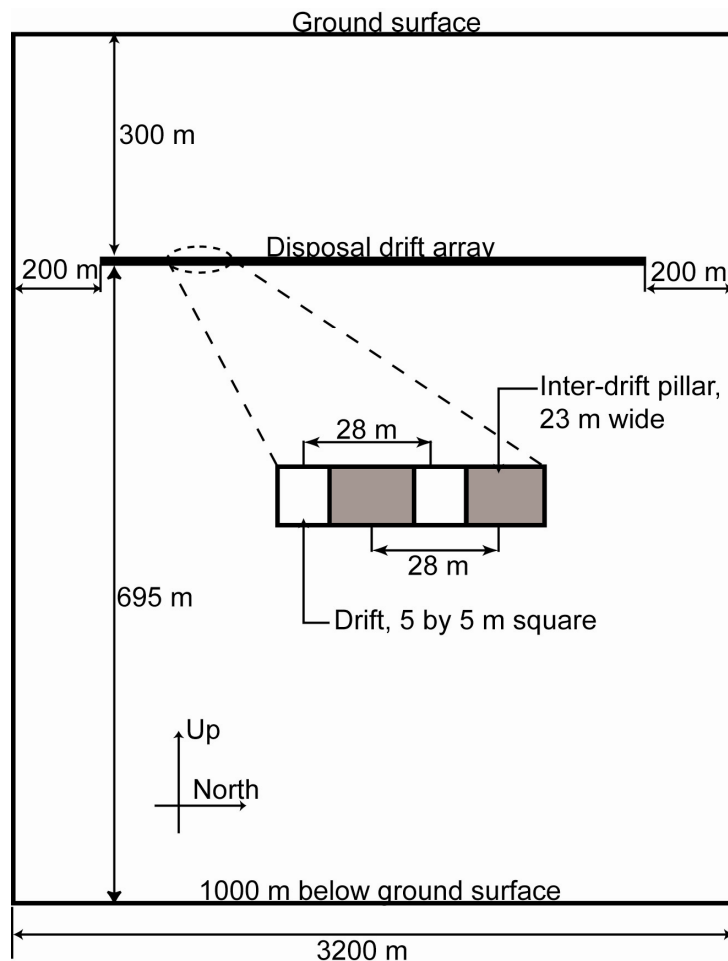


**Figure 3-1. Schematic Illustration of the Site-Scale Model Showing a 2,800-m [9,186 ft]-Wide Disposal Drift Array at a Depth of 300 m [984 ft] Below the Ground Surface**

of 94–114 °C [201–237 °F] simulates approximately the effects of latent heat of vaporization. Mechanical deformation was modeled as elastic-plastic with a rock strength defined in terms of the Drucker-Prager yield criterion. The mechanical parameters are thermal expansivity, which varies with temperature as described in Table 3-1 based on CRWMS M&O (1997c); Poisson's ratio, set to a constant value of 0.21 based on CRWMS M&O (1997c); and Young's modulus, and Mohr-Coulomb friction angle and cohesion, which were assigned spatially variable values using their relationships with the Q rock-mass quality index, based on a procedure Hoek and Brown (1997) described.

Two drift-scale models centered on drift numbers 48 and 85 were set up to represent areas of maximum and minimum Q values. Each drift-scale model extended laterally from the middle of the contiguous south-side pillar to the middle of the contiguous north-side pillar, giving a model width of 28 m [92 ft], as described in Figure 3-2(b). Drift number 48 represents maximum Q, and number 85 represents minimum Q (Figure 2-1). The absolute minimum Q occurs between drift numbers 98 and 99. However, the minimum Q model was set up around drift number 85 to avoid lateral thermal gradients due to end effects, which the site-scale model showed to be strong in the vicinity of drift numbers 98 and 99.

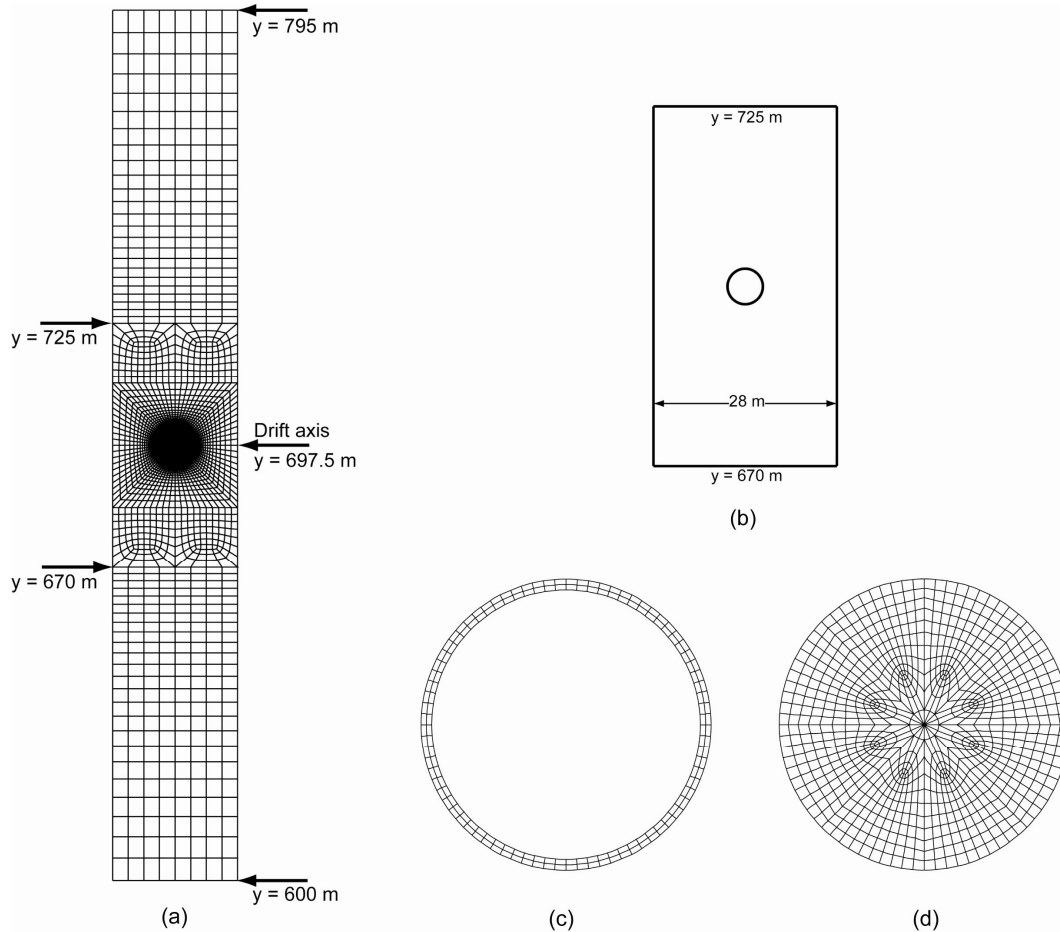


**Figure 3-2. Geometry and Finite Element Discretization of the Drift-Scale Model Showing (a) Entire Drift-Scale Model; (b) a Rectangular Zone of Interest Around a 5-m [16.4-ft]-Diameter Circular Opening, Representing the Drift; (c) Finite Element Model of a 20-cm [7.9-in]-Thick Concrete Liner, Representing Ground Support; and (d) Finite Element Model of the Drift Section, Representing the Excavated Rock. The Vertical Coordinate y Is the Same as “Up” and y = 0 at 1,000 m [3,281 ft] Below the Ground Surface in the Site-Scale Model.**

<b>Table 3-1. Relationship Between Thermal Expansivity and Temperature*</b>	
Temperature °C	Thermal expansivity ( $10^{-6}/K$ )
0.0	5.07
29	5.07
51	7.30
98	7.30
102	8.19
148	8.19
152	8.97
200	8.97

\*CRWMS M&O. “Repository Ground Support Analysis for Viability Assessment.” BCAA00000–01717–0200–00004, Revision 00. LSN Accession Number MOL.19971210.0093. Las Vegas, Nevada: Civilian Radioactive Waste Management System Management and Operating Contractor. 1997.

### 3.3 Initial and Boundary Conditions and Heat Source

The initial temperature was set to 18.7 °C [65.7 °F] at the ground surface and increased with depth at rates of 0.02, 0.018, 0.03, or 0.008 °C/m [0.0034, 0.003, 0.0051, or 0.0014 °F/ft] for depth ranges of 0–150, 150–400, 400–700, and 700–1,000 m [492–1,312; 1,312–2,297; and 2,297–3,281 ft], respectively, based on CRWMS M&O (1997b). The initial vertical stress was determined using an average rock density of 2,274 kg/m<sup>3</sup> [142 lb/ft<sup>3</sup>], which gave a vertical stress of 0.022 MPa/m [0.000973 ksi/ft] of depth below the ground surface. The initial horizontal-to-vertical-stress ratio was set to the zero-lateral-strain value of  $\nu/(1-\nu)$ , where  $\nu = 0.21$  is the Poisson's ratio.

Boundary conditions for the site-scale model (Figure 3-1) consist of fixed initial-value temperature at all exterior boundaries, no lateral displacement at the vertical boundaries, no vertical displacement at the model base, and free surface conditions at the ground surface. Boundary conditions for the drift-scale model [Figure 3-2(a)] were set using temperature and displacement histories calculated in the site-scale model at the drift-scale model exterior boundary nodes.

Thermal load due to disposed nuclear waste was represented using a volumetric heat source applied to the rock volume within each drift section. It was assumed that all disposed waste in the conceptual design would be loaded into the drifts instantaneously at zero time. Therefore, the volumetric heat source was calculated as  $S_h/V_d$ , where  $V_d$  is the total drift volume based on an average drift length of 1,080 m [3,543 ft], as specified in CRWMS M&O (1997b), and  $S_h$  is the total heat output per unit time from all disposed waste. The history of  $S_h$  is plotted in Figure 3-3 using information from CRWMS M&O (1997b, Table V-1).

### 3.4 Analysis Procedure

Each analysis performed using the site-scale or drift-scale model consisted of a heat conduction analysis to calculate temperature distribution histories that were used as input to a mechanical analysis to calculate time-dependent stresses, displacements, and damage (Table 3-2). The heat conduction analysis consisted of two steps. First, a dummy step lasting  $2 \times 10^{-6}$  seconds was performed to synchronize thermal and mechanical analysis times, but no thermal change occurred during the step. Second, a thermal analysis step lasting 150 years was performed to calculate the thermal effects of the volumetric heat source described in Section 3.3.

The mechanical analysis consisted of four steps. The first two steps were isothermal at the initial temperature state and time-independent but assigned a nominal duration of  $1 \times 10^{-6}$  seconds each. The first step was used to establish the initial static equilibrium state under gravitational loading and boundary restraint. Thereafter, drift excavation was simulated during the second step by removing materials within the drift opening {elements within the 5 by 5-m [16.4 by 16.4-ft] squares in Figure 3-1 for the site-scale model or elements shown in Figure 3-2(d) for the drift-scale model} and calculating a new static equilibrium state. The third mechanical step lasted for 150 years. Temperature distribution histories calculated from the thermal analysis were applied during this step and the mechanical response to the temperature distributions was calculated. The fourth step was time independent but was assigned a nominal duration of 1 year. The step was executed based on the thermal state at the end of the third step to explore mechanical effects of ground support degradation over 150 years. To examine

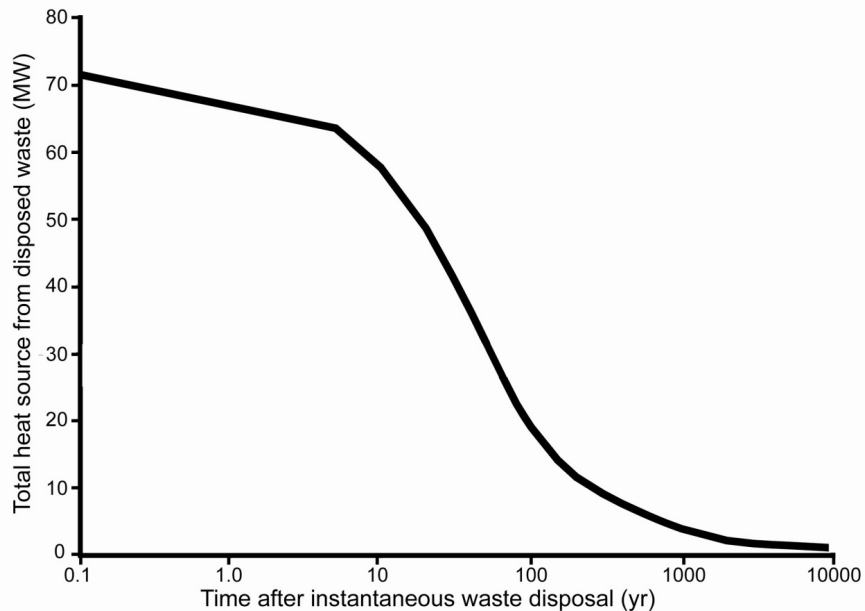


**Figure 3-3. History of Total Heat Source  $S_h$  Used To Represent the Thermal Load of Disposed Nuclear Waste Based on CRWMS M&O (1997b, Table V-1)**

<b>Table 3-2. Sequence of Thermal and Mechanical Analyses</b>		
<b>Time (year)</b>	<b>Thermal Analysis</b>	<b>Mechanical Analysis</b>
$0-1 \times 10^{-6}$	Dummy step—No thermal change	Initial static equilibrium under gravitational loading and boundary restraint—No thermal change
$1 \times 10^{-6}-2 \times 10^{-6}$	Dummy step—No thermal change	Drift excavation simulated with pre-installed ground support. No thermal change
$2 \times 10^{-6}-150$	Thermal analysis step using heat source history in Figure 3-3 as input	Mechanical response with excavated drift and ground support
No time increment	No thermal change from end of previous step	Ground support elements removed during a nominal time period of one year (150–151 years) to simulate degradation of ground support

the effects of ground support degradation on rock damage, elements representing ground support were removed during the step.

## 4 CALCULATED THERMAL-MECHANICAL RESPONSE

The finite element models were used to calculate the effects of waste disposal thermal load on rock temperature, stress, and damage and the effects of rock-mass quality variability on thermally induced mechanical effects. Results of the analysis are described in this chapter.

### 4.1 Host Rock Temperature

Temperature distributions calculated using the site-scale model (e.g., Figures 4-1 and 4-2) indicate that a vertical temperature gradient would develop in the host rock of a nuclear waste repository, such as that modeled, and will likely be sustained for a long time during the heating period. Lateral temperature gradients also may occur, especially close to the ends of the disposal array (Figures 4-1 and 4-2) or within close proximity of the openings through a zone approximately two to three drift diameters above and below the openings [Figure 4-3(b)]. The lateral gradients are likely to be stronger at early times (e.g., Figures 4-1 and 4-2), are likely to weaken as temperature increases (e.g., Figure 4-2), and could strengthen again during the cooling period (not shown in this work). Results calculated using the drift-scale model [Figure 4-3(b)] indicate that the lateral temperature gradients could be sustained for a long time close to the opening and in the interdrift pillar areas near the elevation of the openings. Temperature gradients are important to rock stress as explained in Timoshenko and Goodier (1970, Chapter 13, Article 153) and to rock damage as illustrated by Ofoegbu and Curran (1987).

Temperature distributions calculated using the site-scale and drift-scale models are similar as can be shown by comparing the lower plot of Figure 4-2 against Figure 4-3(a) and using information such as that described in Table 4-1. The comparison indicates that the drift-scale model can be relied upon to simulate the temperature distribution around individual drifts in the disposal array except for approximately five drifts at the north and south ends of the array. Simulating thermal-mechanical behavior near an end drift would entail using a drift-scale model with appropriate boundary conditions for the end drift.

### 4.2 Rock Damage Based on Inelastic Strain

As discussed in Chapter 1, inelastic straining of brittle rocks, such as several types of igneous, metamorphic, and indurated sedimentary rocks, is dominated by cracking. Therefore, inelastic straining is associated with damage because of the effects of cracks on mechanical strength and stiffness and on rock characteristics important to waste isolation, such as hydrologic and transport properties. Intuitively, the damage intensity associated with a given magnitude of inelastic strain should increase as the inelastic strain magnitude increases. Therefore, magnitudes of inelastic strain calculated using a numerical model could be interpreted to indicate relative intensities of damage, without quantifying the damage intensity in terms of crack or fracture density or connectivity. Therefore, for the analyses described in this report, relative damage was described in terms of the Euclidean norm of the inelastic strain tensor accumulated through the simulated history and hereafter referred to simply as “inelastic strain.” Plots of accumulated inelastic strain at 150 years shown in Figures 4-4 through 4-7 indicate that the heat load due to disposed waste could cause rock damage close to the drift openings, especially in the roof and floor areas, and in the interdrift pillars. Potential occurrence of rock damage in the roof and floor of the openings and in the pillars could be explained by considering the effects of the disposal geometry on mechanisms of thermally induced deformation, as

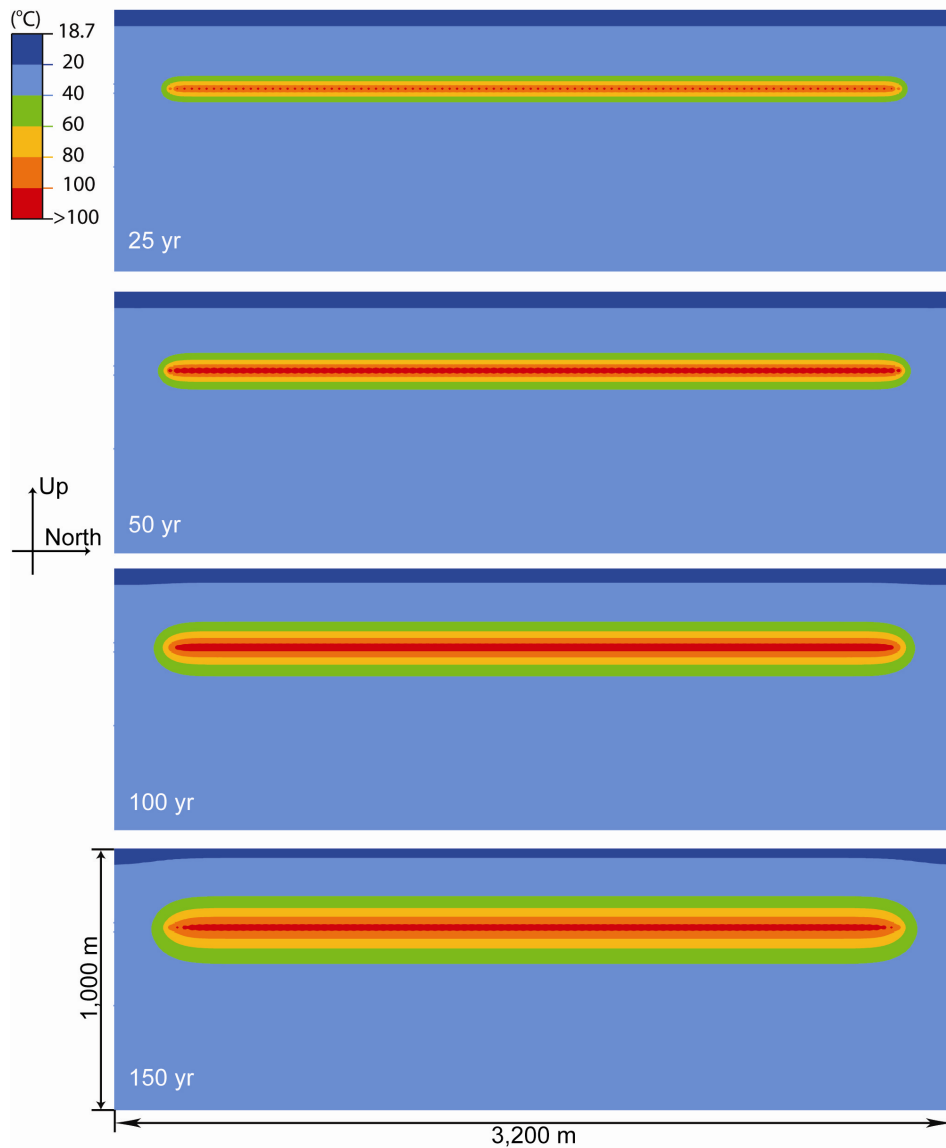


**Figure 4-1. Temperature Distributions Over the Conceptual Disposal Array at 25, 50, 100, and 150 Years After Instantaneous Waste Loading of All Disposal Drifts**

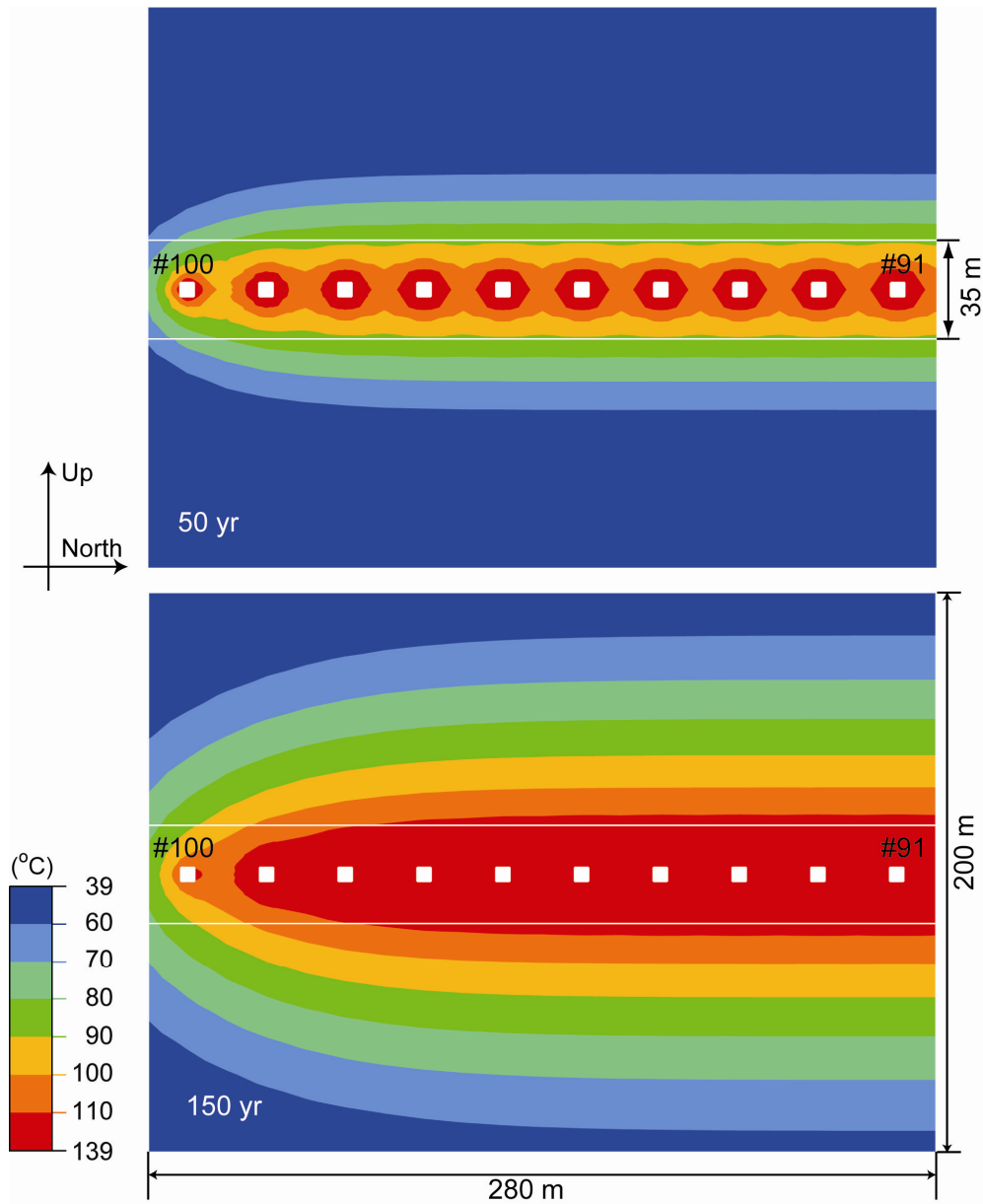


**Figure 4-2. Temperature Distributions Within Approximately 100 m [328 ft] Above and Below the First 10 Disposal Drifts at the South End of the Site-Scale Model (Drifts 91–100) at 50 and 150 Years After Instantaneous Waste Loading of All Disposal Drifts**

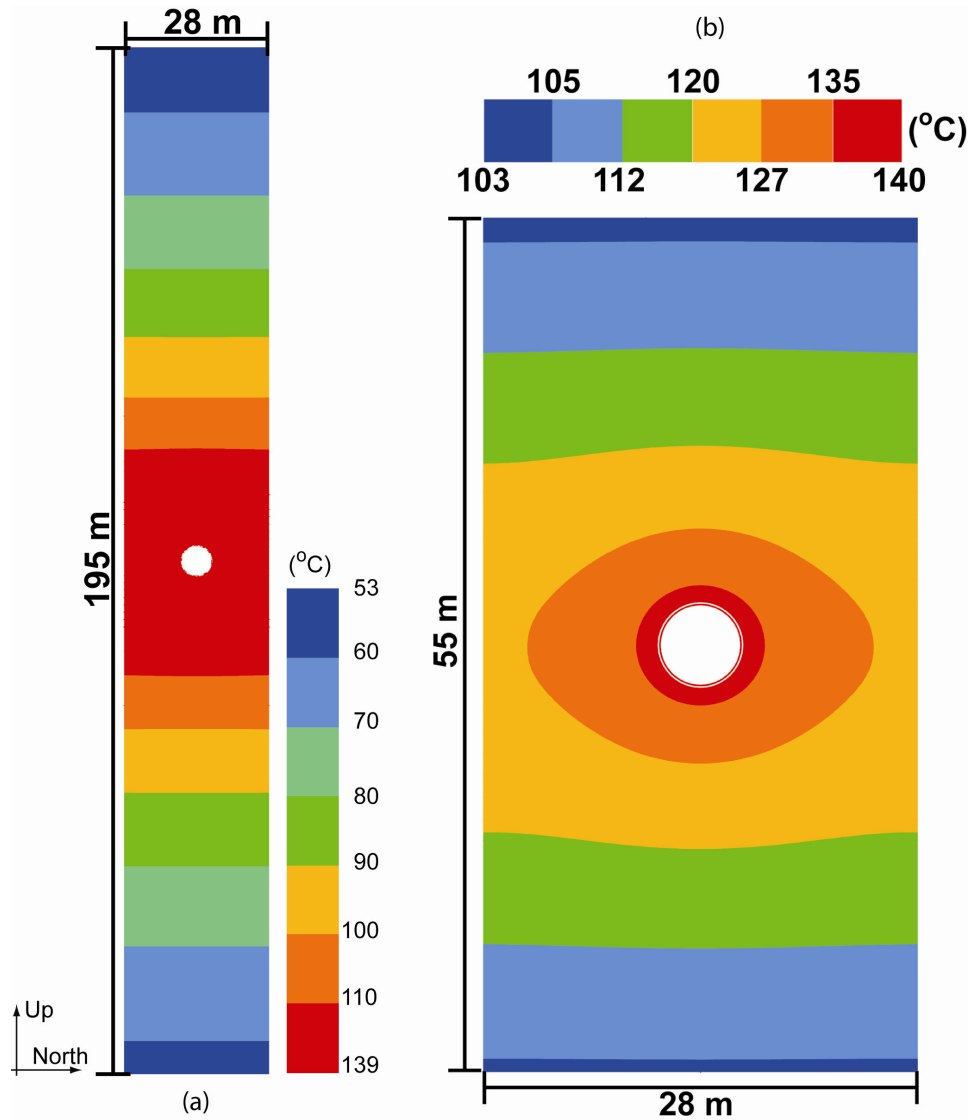


**Figure 4-3. Temperature Distributions Within (a) 95 m [312 ft] and (b) 25 m [82 ft] Above and Below a Drift Based on the Drift-Scale Model at 150 Years After Instantaneous Waste Loading of All Disposal Drifts**

<b>Table 4-1. Vertical Thickness of Rock Subjected to Given Temperature Ranges at 150 Years Based on the Site-Scale (Figure 4-2, lower plot) and Drift-Scale [Figure 4-3(a)] Models</b>		
<b>Temperature Range (°C)</b>	<b>Rock Thickness Based on Site-Scale Model in Figure 4-2, North Boundary of Lower Plot (m)</b>	<b>Rock Thickness Based on Drift-Scale Model in Figure 4-3(a) (m)</b>
110–139	42.8	43.0
100–110	19.2	19.8
90–100	23.5	23.7
80–90	25.7	26.4
70–80	29.9	29.7
60–70	32.1	33.6

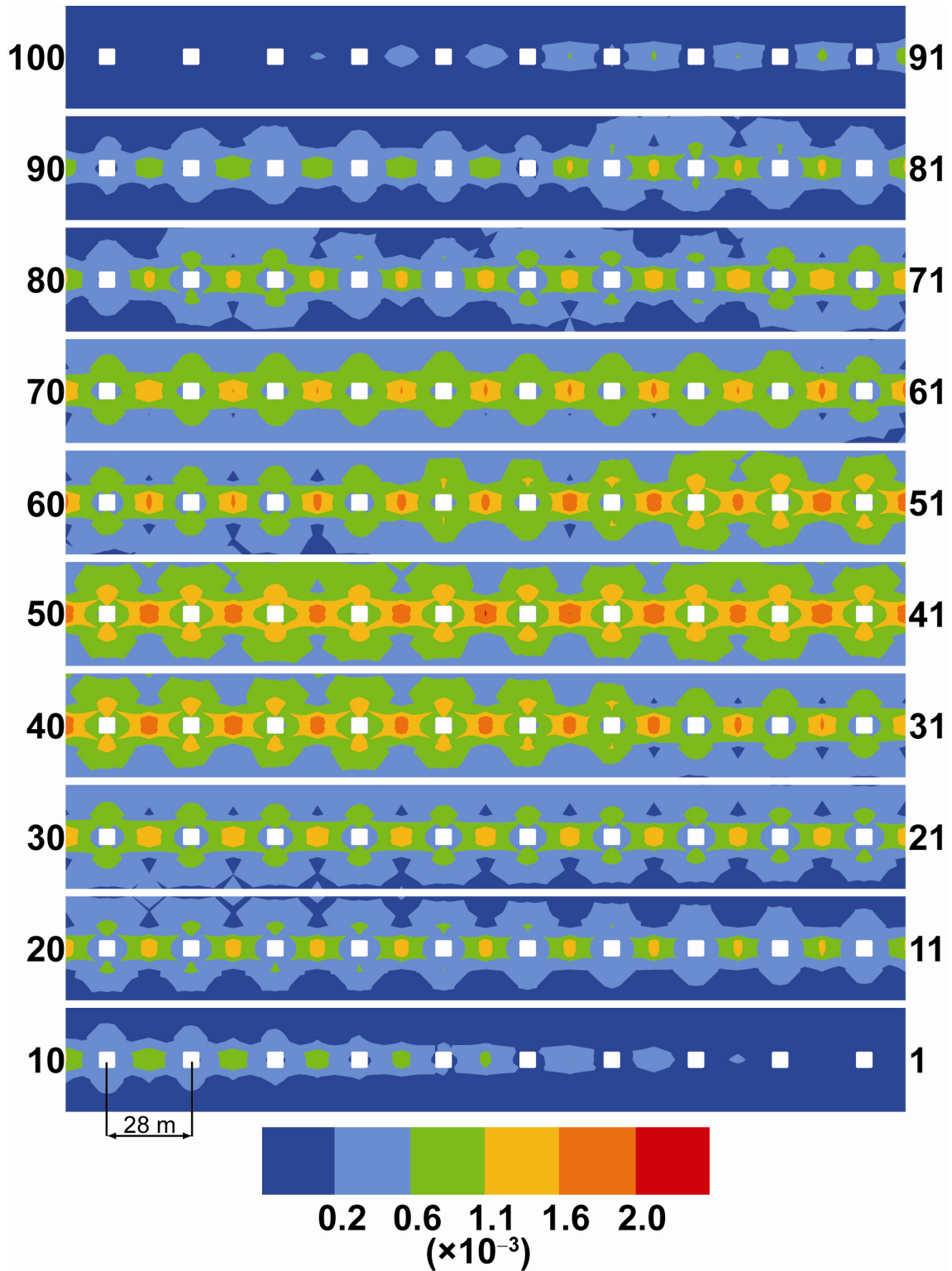


Figure 4-4. Inelastic Strain Distribution at 150 Years for the Case of Drift Openings With Stiff Ground Support. The Plot Arrangement Is the Same as Described in Figure 2-1.

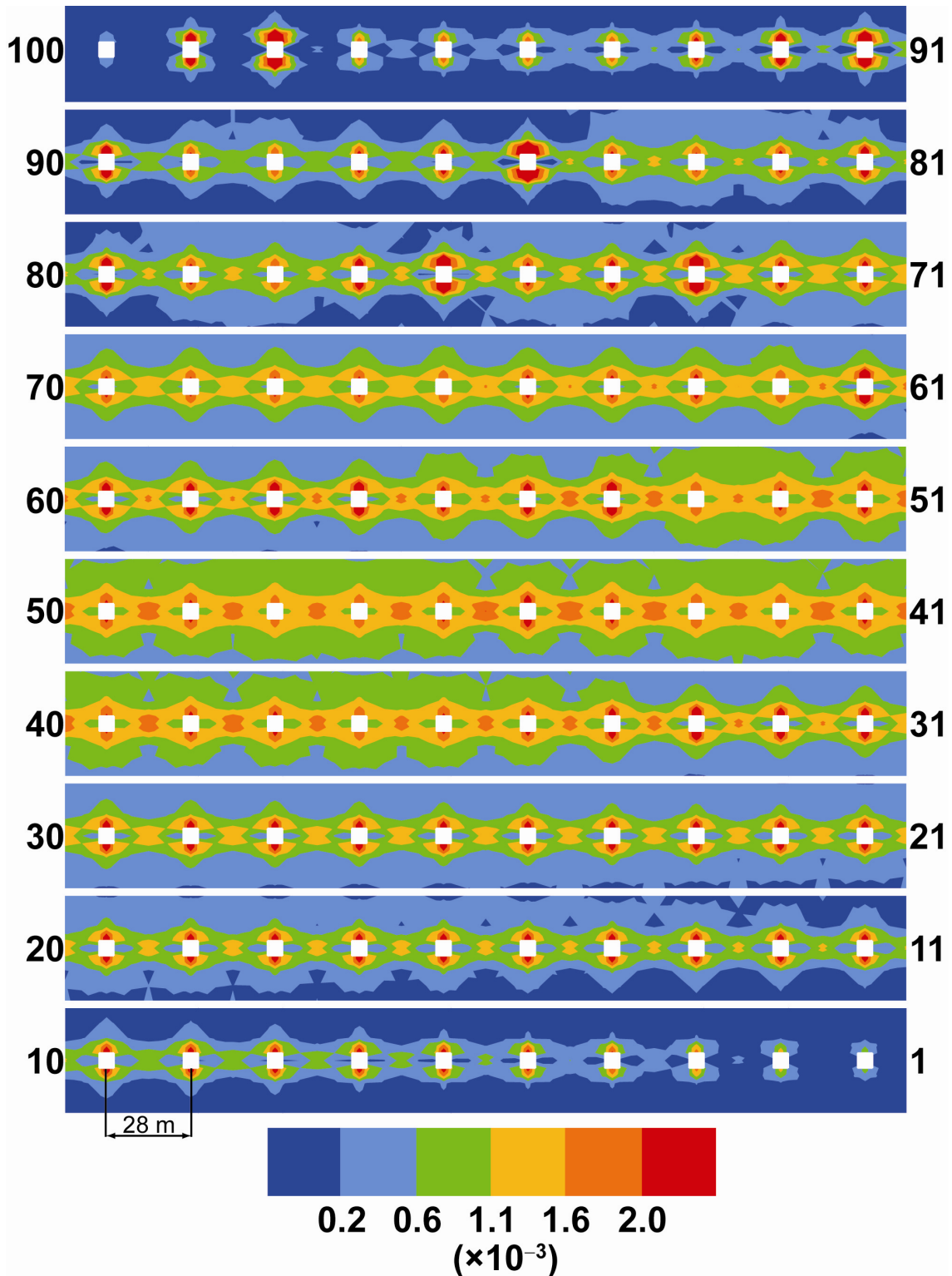


Figure 4-5. Inelastic Strain Distribution at 150 Years for the Case of Drift Openings With Degraded Ground Support. The Plot Arrangement Is the Same as Described in Figure 2-1.

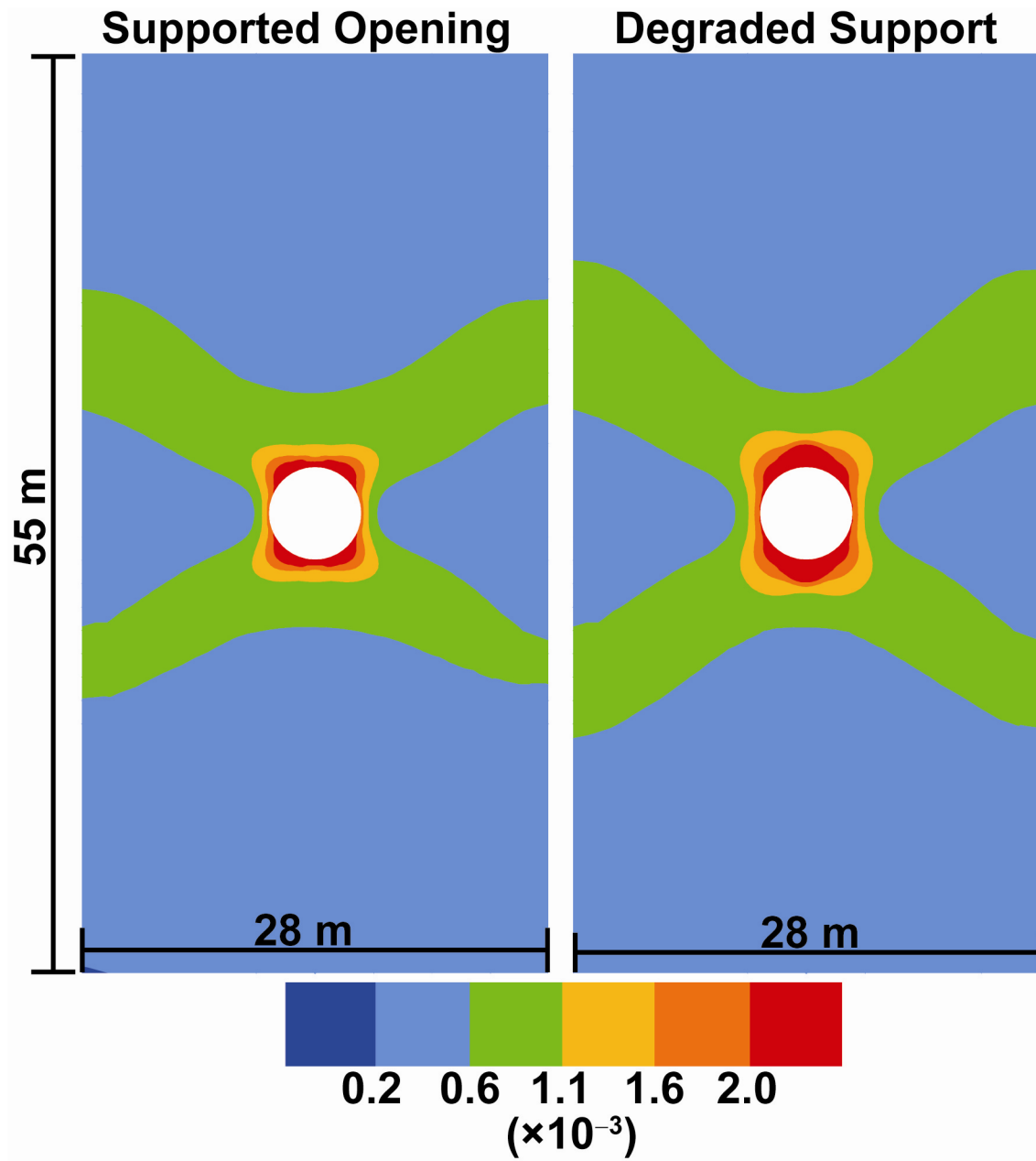
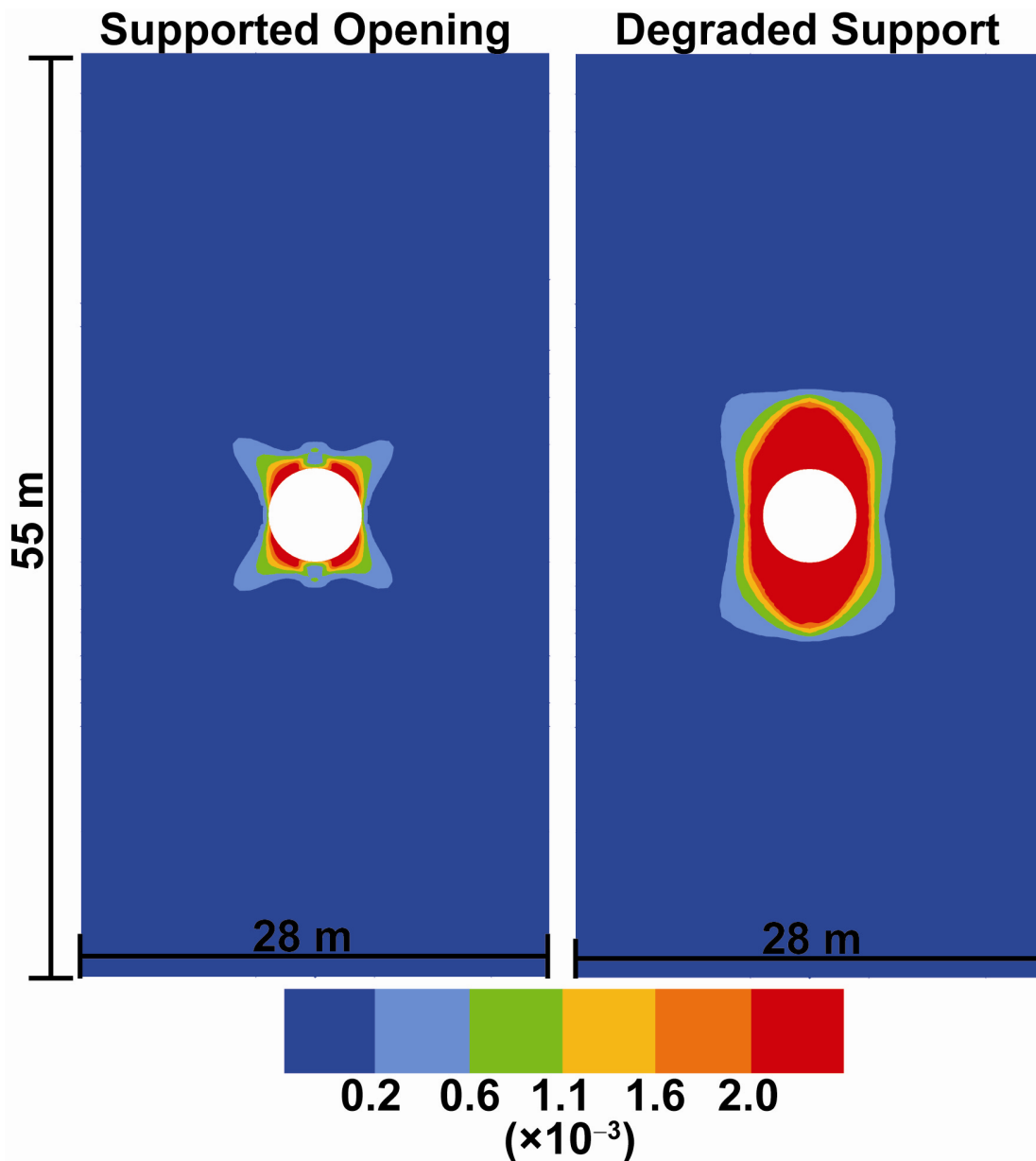
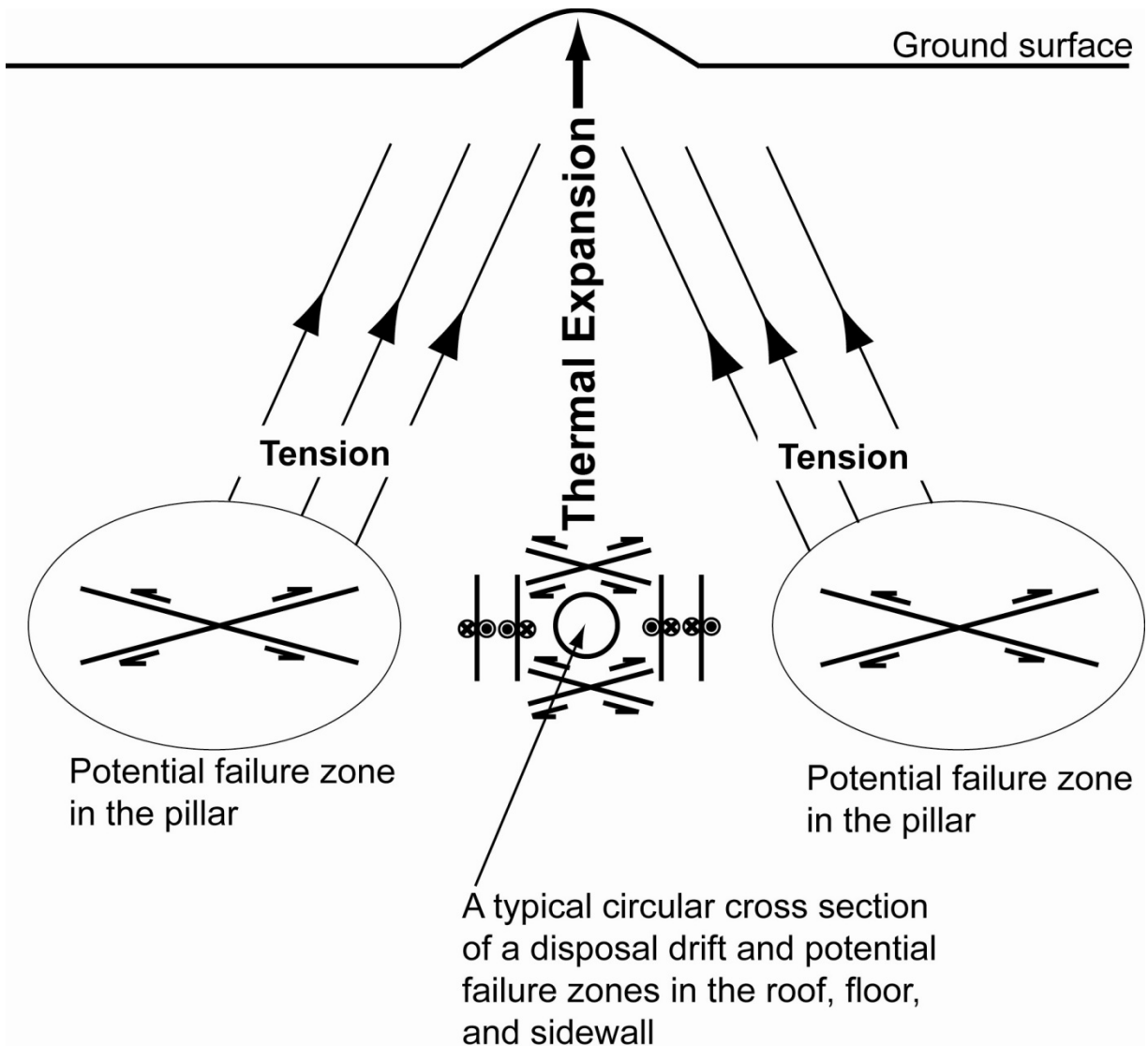


Figure 4-6. Inelastic Strain Distribution at 150 Years Based on the Drift-Scale Model for Areas of High Rock-Mass Quality



**Figure 4-7. Inelastic Strain Distribution at 150 Years Based on the Drift-Scale Model for Areas of Low Rock-Mass Quality**

Ofoegbu (2001) described. The shape of the disposal array and the relative closeness of the ground surface (Figure 3-1) allow a limited amount of upward expansion but negligible expansion downward or laterally. Therefore, rock directly above a typical disposal drift can expand upward more than less heated rock in the pillar and impose an upward drag (tension) on the pillar rock, as illustrated in Figure 4-8. Also, because the disposal array extends laterally much more than vertically and lateral expansion is suppressed more than vertical expansion, the lateral component of thermal stress is much greater than the vertical component. Close to the openings, the effects of the increased lateral stress are reinforced by stress concentrations



**Figure 4-8. Schematic Illustration of Rock Deformation Mechanisms Due to Heat From a Horizontal Array of Fully Loaded Waste Disposal Drifts. The Disposal Thermal Load and Rock-Mass Thermal-Mechanical Properties Determine the Deformation Magnitudes and Type (i.e., Elastic or Inelastic)**

at the roof and floor but diminished by stress concentrations at the sidewalls. These stress conditions, which depend only on the disposal geometry, favor the development of a reverse-faulting style deformation mechanism in the roof and floor areas of the drifts and in the pillars, but a strike-slip faulting style deformation mechanism near the drift sidewall (Figure 4-8).

Whereas the deformation style is determined by the disposal geometry, the magnitude and type (i.e., elastic or inelastic) of deformation are determined by the thermal load and rock-mass mechanical properties. As described in Chapter 1, the thermal load and rock mechanical properties determine the magnitude of thermal stress and whether the stress is sufficient to cause inelastic deformation. Thus, rock damage in the pillars is stress controlled and, therefore, more intense in higher rock-mass quality areas where the rock stiffness is large enough to generate stresses sufficient to cause rock failure. Conditions that increase rock stress will likely increase the potential for pillar damage, more so in higher quality (higher stiffness) than lower

quality (lower stiffness) rock. In contrast, rock damage in the roof and floor, though stress controlled, is influenced by support conditions at the boundaries of the opening. Therefore, the loss of ground support increased damage in the roof and floor, especially in areas of low rock-mass quality. For example, compare the increase in inelastic strain in the roof and floor areas of drift numbers 81–100 between the end of supported-opening conditions (Figure 4-4) and the degraded-support conditions (Figure 4-5). Also, compare the inelastic strain increase between the left and right plots of Figure 4-7 with the hardly noticeable change between the left and right plots of Figure 4-6. As the comparisons show, conditions that reduce confinement at the boundary of an opening will likely increase rock damage in the roof and floor, more in lower quality than in higher quality rock.

Therefore, the disposal thermal load could cause rock damage in the roof and floor of underground openings and in the intervening pillars. Rock damage in the roof and floor could affect the mechanical stability of the openings, is influenced by ground support conditions, and will likely occur more in rock of lower mechanical quality. In contrast, rock damage in the pillar is stress controlled and could occur more in rock of higher mechanical quality. Furthermore, rock damage in the pillar will likely be insufficient to affect mechanical stability of the openings, but could affect water flow (e.g., Ofoegbu, 2001).

### **4.3 Modeling with Single-Valued Rock-Mass Quality Index**

Additional calculations were performed to evaluate the use of single-valued representations of the rock-mass quality index. Analyses were performed using two modified site-scale models with  $Q$  assigned a constant value everywhere.  $Q$  was assigned the minimum value everywhere in one case and the maximum value in the other case. Results calculated using the two model cases were compared with the results described in Section 4.2.

The comparison is illustrated in Figure 4-9 for drift numbers 91–100 and Figure 4-10 for drift numbers 41–50. The comparison could be used to evaluate different approaches for assessing the effects of spatial variability of a parameter, such as  $Q$ , on a response, such as rock damage. Typically, a statistical approach for the assessment may consist of performing analysis with a series of drift-scale models, each assigned a constant  $Q$  value based on a statistical distribution of  $Q$  and averaging the calculated response somehow to obtain a representation of the average response.

For the results in Figures 4-9 and 4-10, the objective of such statistical analysis would be to obtain a representation of case 1(a) using a statistical combination of the results for cases 2(a) and 3(a), or to obtain a representation of case 1(b) using a statistical combination of cases 2(b) and 3(b). As Figures 4-9 and 4-10 indicate, deriving an adequate representation of case 1(a) using 2(a) and 3(a) or case 1(b) using 2(b) and 3(b) will be difficult. However, the adequacy of a representation depends on the intended use of the representation. Figures 4-9 and 4-10 suggest that information based on a statistical model of spatially variable thermal-mechanical response could be evaluated using calculations based on a thermal-mechanical model that includes aspects of the spatial variability of material properties.

### **4.4 Effects of Ground Support on Rock Damage**

A variant of the drift-scale model that does not include ground support was used for additional analysis to explore the effects of ground support on rock damage due to thermal load. In the

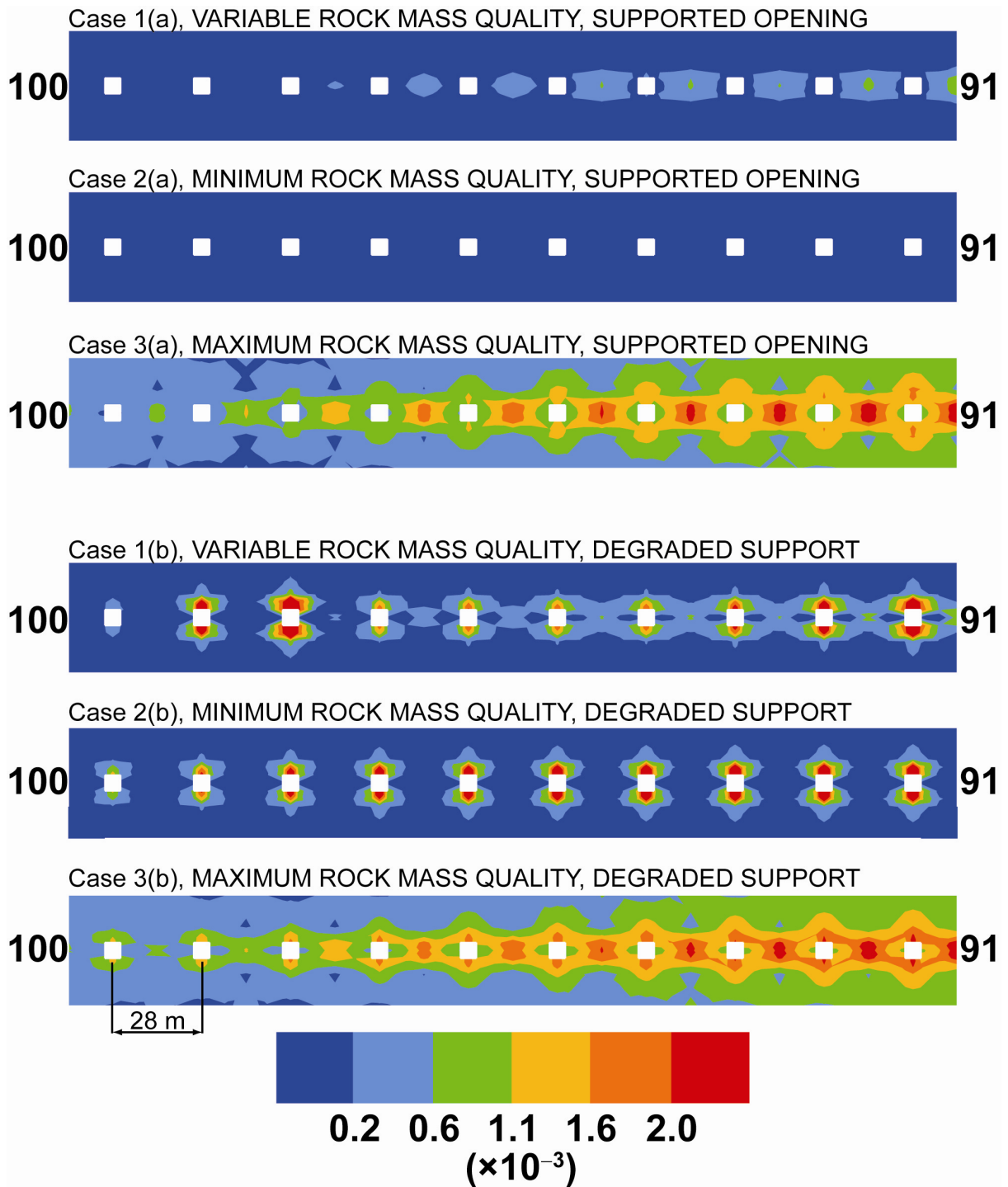


**Figure 4-9. Inelastic Strain Distributions Between Drift Numbers 91–100 (at the South End of the Disposal Array) Calculated Using Three Model Cases: (i) Q Applied as a Spatial Variable as Described in Chapter 2; (ii) Q Assigned the Minimum Value Everywhere, and (iii) Q Assigned the Maximum Value Everywhere. Plots Represent Conditions for (i) Drifts With Stiff Ground Support and (ii) Drifts With Degraded Support.**

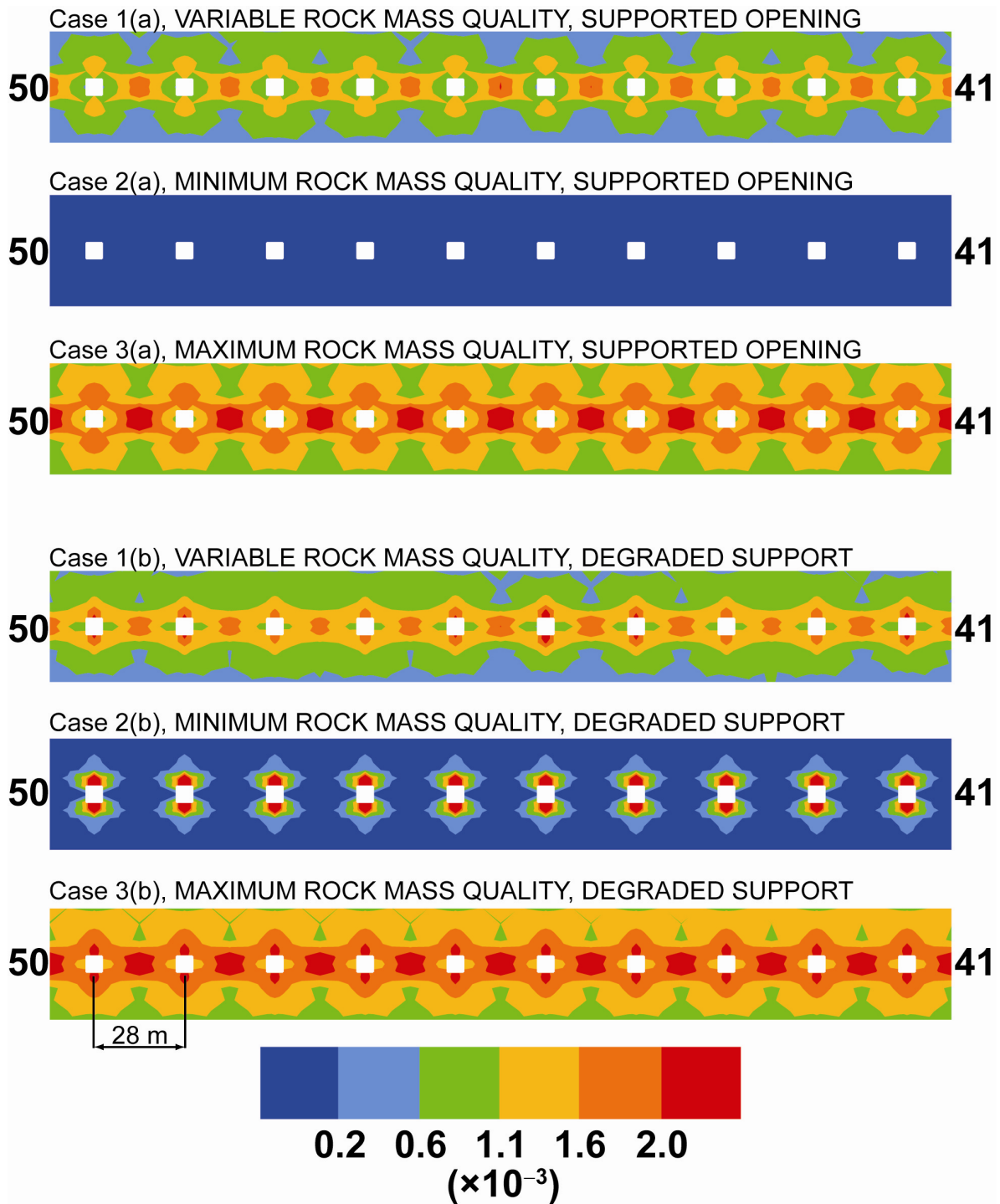


**Figure 4-10. Inelastic Strain Distributions Between Drift Numbers 41–50 (in the Middle of the Disposal Array) Calculated Using Three Model Cases: (i) Q Applied as a Spatial Variable, as Described in Chapter 2, (ii) Q Assigned the Minimum Value Everywhere, and (iii) Q Assigned the Maximum Value Everywhere. Plots Represent Conditions for (i) Drifts With Stiff Ground Support and (ii) Drifts With Degraded Support.**

model variant, the two rings of solid elements originally set up to represent concrete liner [Figure 3-2(c)] were assigned rock properties and fully bonded to surrounding elements. The resulting model represents a 5-m [16.4-ft]-diameter circular opening (same as the other drift-scale models) without ground support. High-Q and low-Q versions of this model variant were implemented, but an analysis using the low-Q variant did not execute to completion, because of numerical instability associated with excessive inelastic deformation at approximately 1 year after instantaneous waste loading.

Typical displacement histories calculated using the high-Q, nonsupported drift model variant (Figure 4-11) indicate that thermal loading caused the simulated drift to displace southward and upward. The calculated displacements included a drift convergence (decrease in diameter) of approximately 20 mm [0.79 in]. The horizontal convergence occurred quickly during the first approximately 20 years and remained constant thereafter. The vertical convergence, in contrast, occurred more slowly but reached a constant value after approximately 50–60 years. The convergence due to excavation {approximately 0.2 mm [0.0079 in] horizontal and 1.8 mm [0.071 in] vertical} is negligible relative to the convergence due to thermal load, as Figure 4-11 indicates.

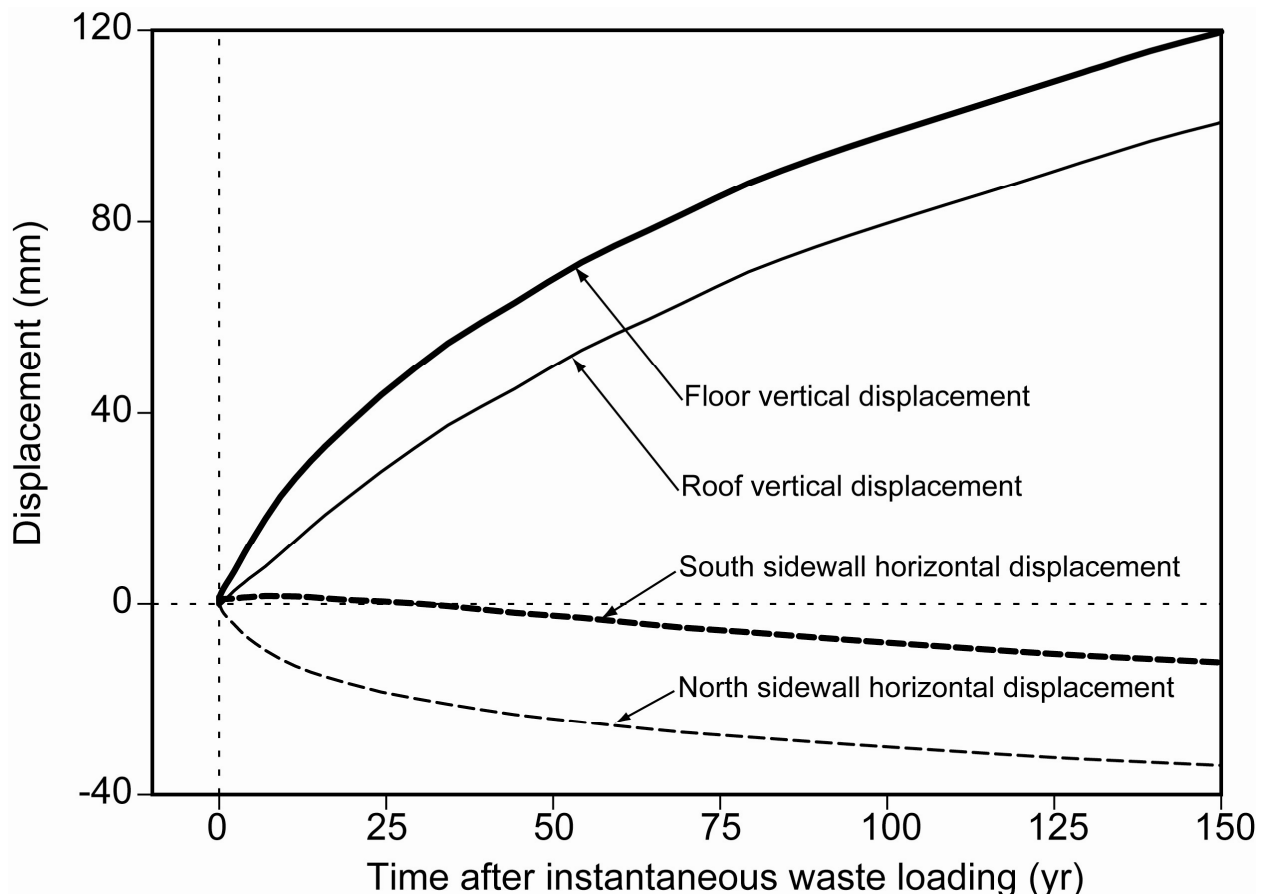


**Figure 4-11. Displacement History at the Roof, Floor, and North and South Sidewalls of a Disposal Drift Without Ground Support Based on a Drift-Scale Model Analysis for High-Q Areas. Vertical Displacement Is Positive Upward, and Horizontal Displacement Is Positive Northward.**

The inelastic strain distribution calculated for the unsupported opening through 150 years is compared (Figure 4-12) with the inelastic strain distributions calculated for an opening with ground support, before and after removal of the support elements (as described in Section 3.4) to simulate support degradation. The results indicate that a concrete-liner ground support likely will not affect pillar damage but will have appreciable effects on rock damage close to the drift opening. This calculated result is consistent with the expected effects of a concrete-liner ground support on stress conditions. A concrete liner applies stress directly at the edge of the opening, thereby creating a confining condition that decreases rock failure near the opening.

In contrast, the zone of influence of the concrete-liner stress does not extend far enough into the rock to have any effect on stress-controlled rock failure in the pillar. Therefore, a concrete-liner ground support could reduce rock damage near the opening but is not likely to affect rock damage in the pillar. In general, a ground support system could affect rock damage only within the mechanical influence zone of the ground support system.

#### **4.5 Potential Loading of a Concrete Liner Ground Support**

The drift-scale model setup included documentation of the concrete-liner pressure history through each analysis. Concrete liner pressure may result from suppressed inelastic deformation of the rock or suppressed thermal expansion of the liner or rock. For example, the calculated maximum inelastic strain magnitude was 3.78 microstrain for a high-Q model with concrete-liner ground support and 13.5 microstrain for the same model without ground support. This difference, which is also described in Figure 4-12, indicates that potential inelastic deformation of rock adjacent to a thermally loaded drift could be suppressed by ground support, such as a concrete liner. The ground support element would be subjected to loading due to the suppressed inelastic deformation. Additional loading of the ground support may result from suppressed thermal expansion of the support element or surrounding rock.

As shown in Figures 4-13 through 4-15, the concrete-liner pressure may vary around the liner circumference and could be affected by the rock-mass mechanical properties. Generally, the lowest Q model gave a greater concrete-liner pressure than the highest Q model. Because the pressure due to suppressed thermal expansion of the liner or rock should be greater in the highest Q than lowest Q model,<sup>1</sup> the greater concrete-liner pressure in the lowest Q model indicates that suppressed inelastic deformation is the prevalent cause of concrete-liner pressure in the models.<sup>2</sup>

The liner pressure also is affected by frictional resistance at the liner–rock interface, as illustrated in Figure 4-15. Generally, liner pressure approaches a hydrostatic (i.e., equal all around) distribution as the liner–rock interface approaches frictionless. The liner pressure decreases in the roof and floor areas and increases in the sidewalls as the liner–rock friction coefficient decreases. For non-zero friction, the liner pressure in the roof and floor exceeds the liner pressure in the sidewalls by an amount that increases as the friction coefficient increases.

A model that assumes the liner is bonded to the rock will give a maximum value for the liner pressure in the roof and floor and a minimum value in the sidewalls.

---

<sup>1</sup>Both models have the same temperature distribution and concrete-liner properties, but the rock-mass stiffness is greater in the highest Q model than in the lowest Q model. Therefore, pressure due to suppressed thermal expansion of the liner or rock should be greater in the highest Q model.

<sup>2</sup>As discussed in Section 4.2 and illustrated in Figures 4-5 and 4-7 (compared with 4-6), greater inelastic deformation will occur adjacent to a heated drift in lower Q than in higher Q areas.

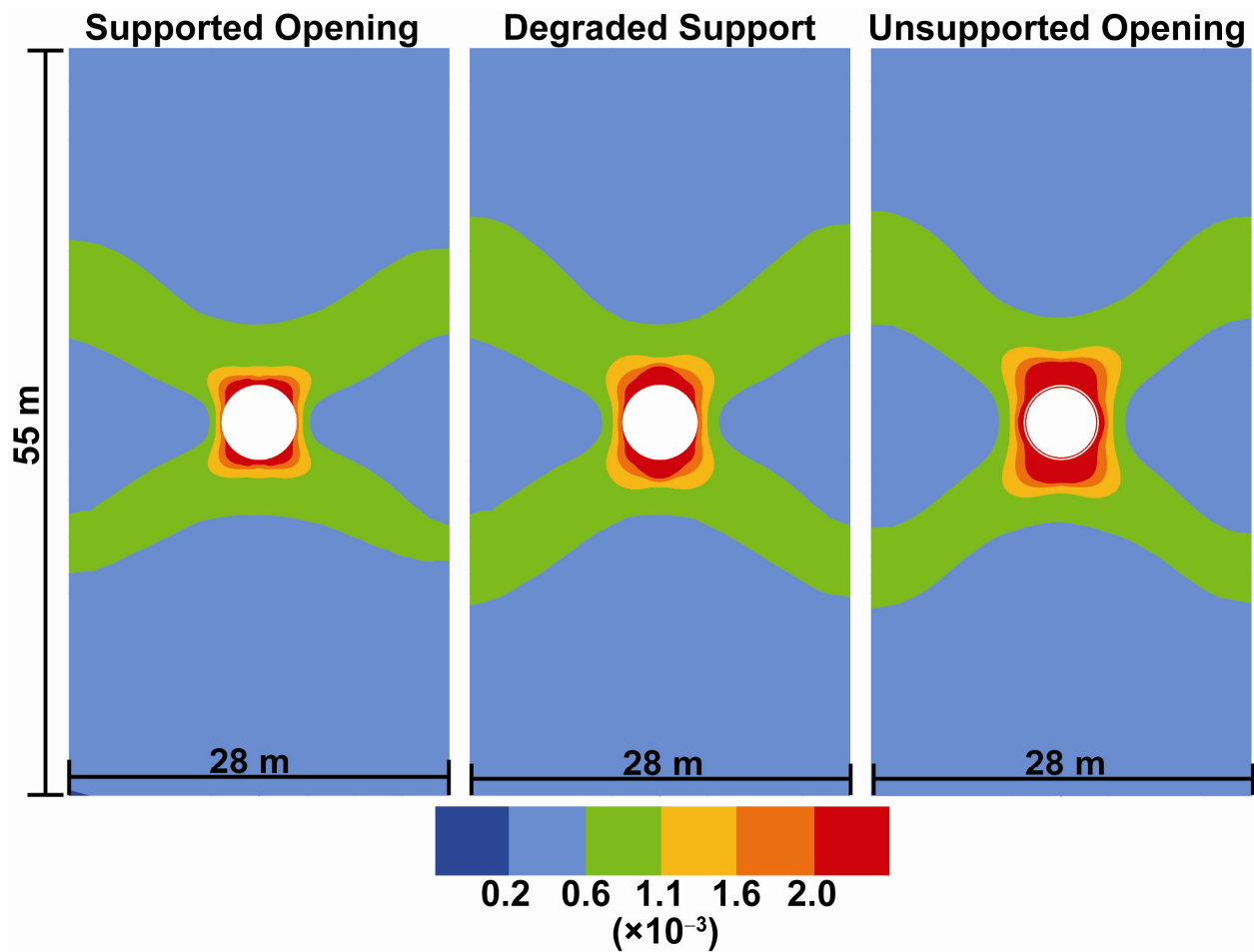


**Figure 4-12. Inelastic Strain Distributions at 150 Years Based on Drift-Scale Modeling for High-Q Areas, Showing the Effects of Ground Support on Thermally Induced Rock Damage. Results Are Shown for Cases of Supported Opening, Degraded Support (Simulated by Removing Elements After 150 Years), and No Ground Support for the Simulated 150-Year Period.**

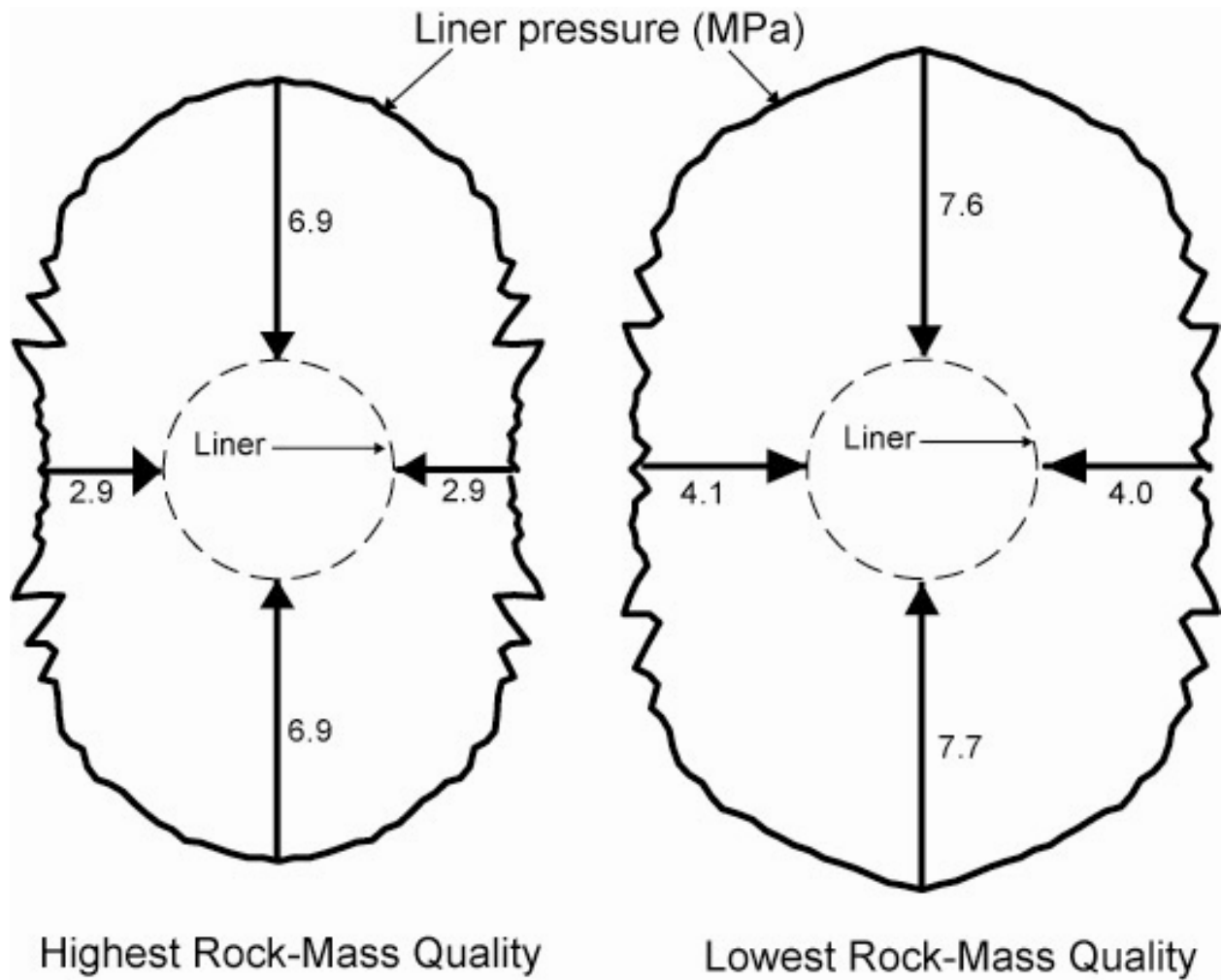


**Figure 4-13. Distribution of Liner Pressure Around a Drift Circumference at 150 Years After Instantaneous Waste Loading, Based on Highest Q and Lowest Q Drift-Scale Models With Liner Fully Bonded to Rock. The Magnitude of Liner Pressure Is Plotted as a Proportional Radial Distance from the Liner–Rock Interface.**

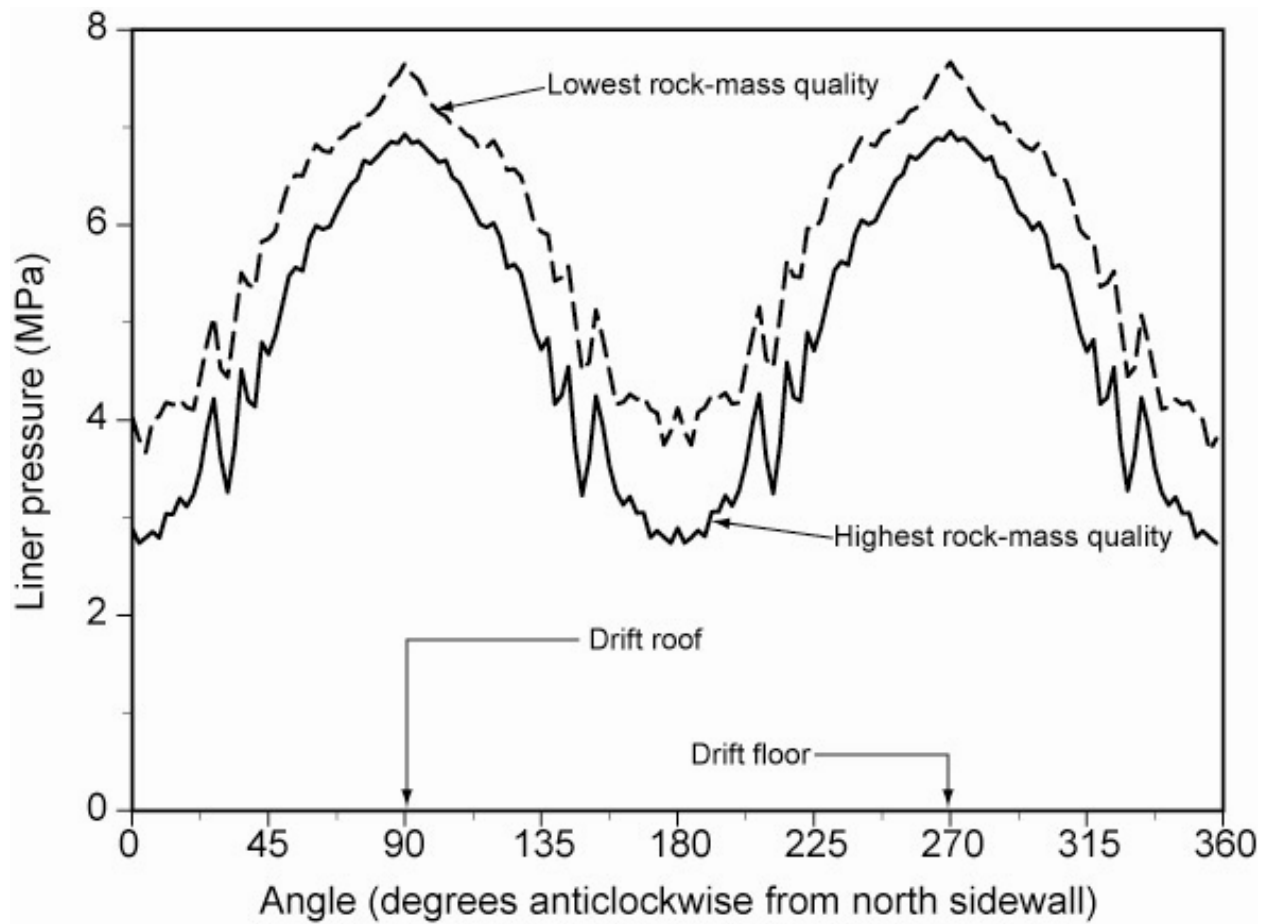


**Figure 4-14. Variation of Liner Pressure With Angular Distance Around a Drift Circumference at 150 Years After Instantaneous Waste Loading, Based on Highest Q and Lowest Q Drift-Scale Models With Liner Fully Bonded to Rock.**

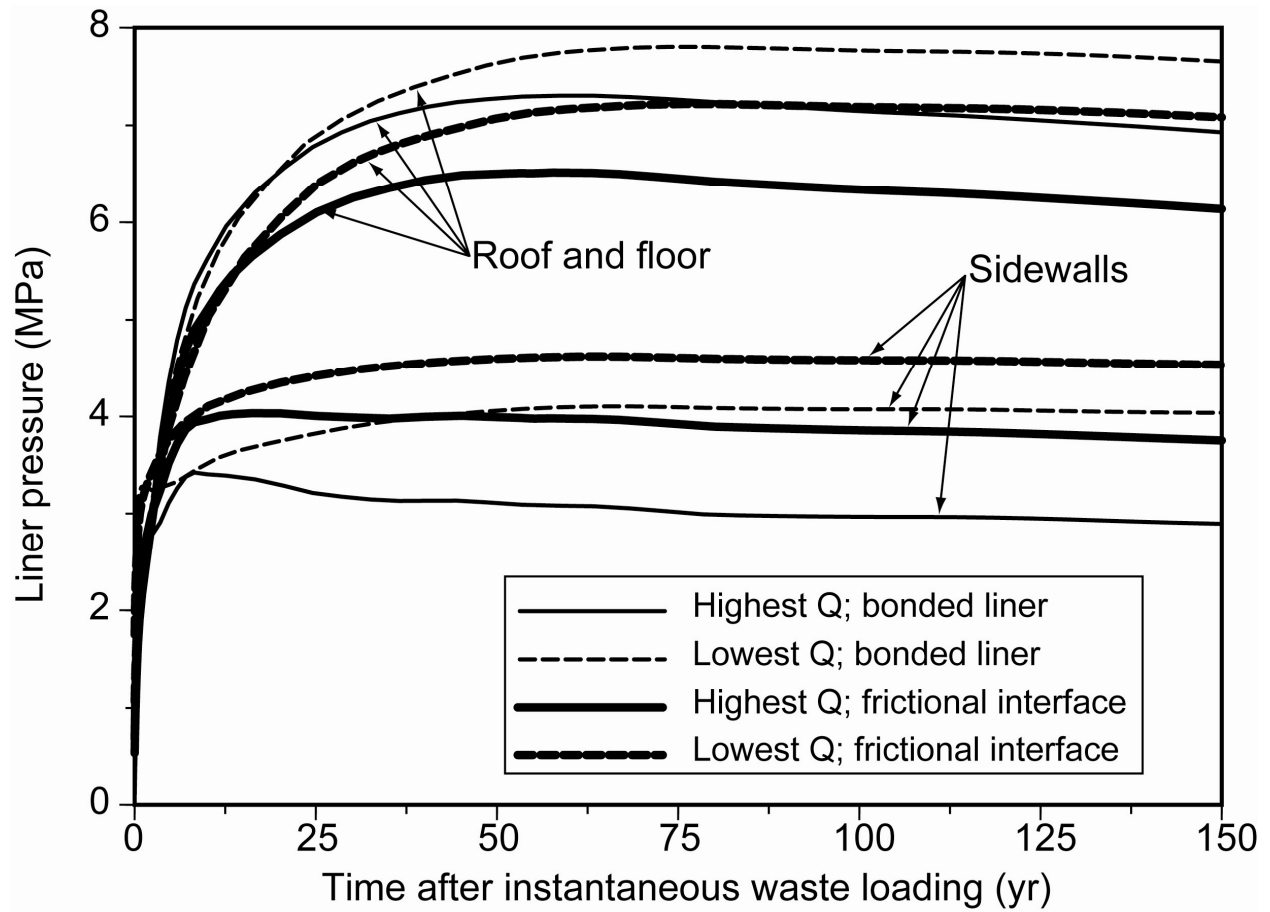


**Figure 4-15. Effects of the Liner–Rock Interface Model on the Calculated Liner Pressure Showing Results for a Fully Bonded Interface Model and a Frictional-Interface Model With a Friction Coefficient of 0.6.**

## 5 SUMMARY OF INSIGHTS

Thermal-mechanical analyses of a conceptual waste disposal design were performed using a series of site-scale and drift-scale models to examine characteristics of potential rock-mass mechanical response to the repository thermal load. The site-scale models included a representation of spatial variability of mechanical properties based on sitewide fracture mapping and were used to examine variability of mechanical response over the disposal area. The drift-scale models, in contrast, allowed a closer examination of the response at the scale of an individual disposal opening. Insights based on the analyses are summarized as follows.

The results indicate the occurrence of a strong vertical temperature gradient in the host rock centered at the disposal horizon. The vertical temperature gradient will likely be sustained through the heating period. A weaker lateral temperature gradient also will occur, especially close to the disposal openings and near the lateral boundaries of the disposal zone. Temperature gradients control development of stress conditions that could cause rock damage.

Rock damage due to thermal load could occur in the roof and floor areas of the disposal openings and in the intervening pillars. Rock damage in the roof and floor could be reduced with appropriate ground support and is likely to occur more in rock of lower mechanical quality. However, ground support is not likely to affect potential rock damage in the pillar, because such damage is driven by stress conditions outside the influence zone of typical ground support. Because of the stress control, rock damage in the pillar could occur more in rock of higher mechanical quality.

A site-scale thermal-mechanical model could provide insights regarding the effects of spatial variability of mechanical properties and a means of evaluating models of spatial variability of mechanical response based on statistical analysis of responses calculated using constant-property mechanical models.

An underground opening used for nuclear waste disposal could be stabilized using ground support designed to reduce inelastic deformation of the rock and, therefore, withstand loading due to suppressed inelastic deformation in addition to loading due to thermal expansion of the rock and support system. The magnitude of such loading can be calculated through numerical thermal-mechanical modeling.

## 6 REFERENCES

Anderson, J.C. "Rock-Mass Response to Coupled Mechanical Thermal Loading, Aspö Pillar Stability Experiment, Sweden." Doctoral Thesis. Royal Institute of Technology, Department of Civil and Architectural Engineering. Stockholm, Sweden. 2007.

CRWMS M&O. "ESF Design Confirmation Task 3, Confirmation of Empirical Design Methodologies." BABEE0000-01717-5705-00002. Rev. 00. LSN Accession Number MOL.19980219.0104. Las Vegas, Nevada: Civilian Radioactive Waste Management System Management and Operating Contractor. 1997a.

———. "Repository Thermal Loading Management Analysis." B00000000-01717-0200-00135. Rev. 00. LSN Accession Number MOL.19971201.0591. Las Vegas, Nevada: Civilian Radioactive Waste Management System Management and Operating Contractor. 1997b.

———. "Repository Ground Support Analysis for Viability Assessment." BCAA00000-01717-0200-00004. Rev. 00. LSN Accession Number MOL.19971210.0093. Las Vegas, Nevada: Civilian Radioactive Waste Management System Management and Operating Contractor. 1997c.

DOE. "Viability Assessment of a Repository at Yucca Mountain. Volume 2: Preliminary Design Concept for the Repository and Waste Package." Las Vegas, Nevada: U.S. Department of Energy. 1998.

Hoek, E. and E.T. Brown. "Practical Estimates of Rock-Mass Strength." *International Journal of Rock Mechanics & Mining Sciences*. Vol. 34. pp. 1,165-1,186. 1997.

Ofoegbu, G.I. "Hydrological Implications of Thermally Induced Geomechanical Response at Yucca Mountain, Nevada." *Rock Mechanics in the National Interest, Proceedings 38<sup>th</sup> U.S. Rock Mechanics Symposium*. D. Elsworth, J.P. Tinucci, and K.A. Heasley, eds. Lisse, Netherlands: A.A. Balkema. 2001.

Ofoegbu, G.I. and J.H. Curran. "Rotation of Principal Stresses Near a Heated Fracture in a Bituminous Sand." *Canadian Geotechnical Journal*. Vol. 24. pp. 357-365. 1987.

Timoshenko, S.P. and J.N. Goodier. *Theory of Elasticity*. Third Edition. New York City, New York: McGraw-Hill. 1970.

Tsang, C.-F., F. Bernier, and C. Davies. "Geohydromechanical Processes in the Excavation Damaged Zone in Crystalline Rock, Rock Salt, and Indurated and Plastic Clays in the Context of Radioactive Waste Disposal." *International Journal of Rock Mechanics & Mining Sciences*. Vol. 42. pp. 109-125. 2005.